Department of Chemistry
University of Helsinki
Helsinki, Finland

STUDIES ON ATOMIC LAYER DEPOSITION OF GOLD AND SILVER THIN FILMS

Maarit Mäkelä
(née Kariniemi)

ACADEMIC DISSERTATION

To be presented, with the permission of the Faculty of Science of the University of Helsinki, for public examination in auditorium A110 of the Department of Chemistry (Chemicum), A. I. Virtasen aukio 1, on June 4th 2018, at 12 o´clock noon.

Helsinki 2018

Supervisor

Professor Mikko Ritala
Department of Chemistry
University of Helsinki
Helsinki, Finland

Reviewers

Professor Erwin Kessels
Department of Applied Physics
Eindhoven University of Technology
Eindhoven, Netherlands

Professor Paul Chalker
Department of Mechanical, Materials and Aerospace Engineering
University of Liverpool
Liverpool, United Kingdom

Opponent

Associate Professor Henrik Pedersen
Department of Physics, Chemistry and Biology
Linköping University
Linköping, Sweden

ISBN 978-951-51-4307-5 (pbk.)
ISBN 978-951-51-4308-2 (PDF)

Unigrafia
Helsinki 2018

Abstract

Atomic layer deposition (ALD) is a thin film deposition method. Typically, an ALD thin film is deposited on a substrate in a heated reaction chamber in vacuum by exposing the substrate to ALD precursors. Commonly a metal precursor and a co-reactant, either an oxidizing or a reducing agent, are used. The film growth in ALD is self-limiting. Thickness of the film can be precisely controlled. ALD thin films are also conformal meaning that the films mimic the structures of the substrates. Plasma-enhanced ALD (PEALD) is an energy enhanced version of thermal ALD. The use of highly reactive radicals instead of the thermal co-reactant is the main difference between the thermal and plasma-enhanced ALD processes. The main drawback of PEALD is issued to be poor conformality of the PEALD thin films caused by the recombination of the radicals on the walls of the nanostructures.

Potential applications of silver and gold thin films deposited by ALD include photonics, catalysis and electronics among others. In these applications conformal thin films with precisely controlled thickness are wanted. The main aim of this study was to develop thermal or plasma-enhanced ALD processes for these metals. Literature survey showed that there exist only a few ALD processes of silver and one PEALD study of gold. The main reason for the small number of processes has been the lack of thermally stable metal precursors. In ALD it is essential to have a thermally stable precursor to ensure the self-limiting growth. During this study several silver and gold compounds were evaluated for ALD. One silver, gold(I) and gold(III) precursor were chosen for the ALD experiments. The silver precursor was applied with plasma-activated hydrogen in a PEALD process and with a reducing agent in a thermal process. It exhibited self-limiting growth in both processes. An ALD gold process was developed with the gold(III) precursor applied with an oxidizing agent. The gold(I) precursor applied with a reducing agent produced pure gold thin films, but no self-limiting ALD process was established.

The other aim of the study was to apply the silver PEALD process to two potential applications as case studies. Surface enhanced Raman scattering (SERS) substrates were coated with silver. Raman intensity of the adsorbed molecules on the silver surface was studied. Significant enhancement in the Raman response of the molecules on the SERS substrates was shown when compared to a neat solution. In the second study, the Ag process was applied to coat titanium dioxide nanotubes and nanoneedles on titanium implants. The silver nanoparticles on implants created an antimicrobial response. In both studies the main advantage of applying ALD was that the amount of silver deposited was precisely controlled.

Preface

The experimental work for this thesis was done during the years 2010-2016 in the Laboratory of Inorganic Chemistry of the University of Helsinki. It has been a privilege to part of the ALD group led by Professors Mikko Ritala and Markku Leskelä. I thank them for giving me a chance to work in their group and to learn from the best ALD experts of the world. I am especially grateful to my supervisor Prof. Mikko Ritala for your guidance, insights and support with my research.

I wish to thank the reviewers of this dissertation, Prof. Paul Chalker and Prof. Erwin Kessels, for their constructive comments regarding my work.

I express my gratitude to all the co-authors. I wish to thank D.Sc. (Tech.) Jaakko Niinistö for being my tutor to the world of ALD. I think every PhD student should have a tutor like you- I was privileged. I thank D.Sc. (Tech.) Matti Putkonen for giving me a chance to participate the conformality study. I also appreciate our discussions about being a researcher. I thank Doc. Marianna Kemell and Dr. Marko Vehkamäki for guidance with FESEM imaging and EDS analysis, and Marko for guidance with FIB-SEM. Prof. Timo Sajavaara, Prof. Jyrki, Räisänen, Dr. Kenichiro Mizohata and Dr. Kristoffer Meinender are thanked for film composition analyses. I wish to thank Mr. Timo Hatanpää for development and synthesis of ALD precursors. I look up to your innovative mind. I wish to thank Dr. Joshua Caldwell and Dr. Aleksandra Radtke and all the co-authors for giving me a chance to participate studies where PEALD Ag was applied to two potential applications. All the former colleagues are thanked for their help and for creating a pleasant work environment.

The research leading to this thesis received funding from the Academy of Finland (Finnish Centre of Excellence in Atomic Layer Deposition).

I am deeply grateful to my parents, Inkeri and Pekka, and to my brother Ville and his family, Viivi, Vuokko and Valtteri, for always supporting me and my family. Also Perhepäiväkoti Viikari is thanked for taking care of my daughter and giving me a peace of mind to work. My best friends, members of “Marttakerho”, are thanked for their support and sympathy during the years. I also wish to thank my husband´s family for taking my part of the gang. I have to mention also my relatives and especially the late Elli Kariniemi, and my godparents Arja-Leena and Veikko Kariniemi, for being role models in the sciences. Finally, I would like to express my gratitude to my daughters, Pihla and Kerttu, you are my reason to live for, and to my husband Juha, you give me strenght. Every chapter comes to an end, but after ends, the following pages open. In every end, there is also a beginning.

CONTENTS

2.1 Atomic layer deposition 17

2.2 Plasma-enhanced atomic layer deposition 23

2.3 Potential applications of silver and gold thin films deposited by ALD 31

2.4 Atomic layer deposition processes of silver and gold thin films 36

2.4.1 Possible pathways to atomic layer deposition of silver and gold thin films 36

2.4.2 Silver ALD processes 38

2.4.3 Gold ALD processes 44

3.1 Precursor characterization 47

3.2 Thin film deposition 47

3.3 Thin film characterization 50

4.1 Silver 51

4.2 Gold 64

4.2.1 $Me_2Au(S_2CNEt_2)$ as a precursor 67

4.2.2 $Au(N(SiMe_3)_2)(PEt_3)$ as a precursor 71

4.3 Application of the developed Ag PEALD process to two case studies 76

4.3.1 Case study 1: Surface Enhanced Raman Spectroscopy 76

4.3.2 Case study 2: Titanium implants 79

List of original publications

This doctoral dissertation consists of a summary and publications, which are referred to in the text by their Roman numerals. The author´s contributions are described in the indentations.

I **Plasma-enhanced atomic layer deposition of silver thin films**

Maarit Kariniemi, Jaakko Niinistö, Timo Hatanpää, Marianna Kemell, Timo Sajavaara, Mikko Ritala, Markku Leskelä
Chem. Mater. **23** (2011) 2901.
The author made the deposition experiments and performed the FESEM, EDS and GIXRD analyses and evaluated the electrical properties of the films. The author wrote the first draft and finalized the paper together with other co-authors.

II **Conformality of remote plasma-enhanced atomic layer deposition processes: An experimental study**

Maarit Kariniemi, Jaakko Niinistö, Marko Vehkamäki, Marianna Kemell, Mikko Ritala, Markku Leskelä, Matti Putkonen
J. Vac. Sci. Techol. A. **30** (2012) 01A115.
The author made the deposition experiments of the Ag thin films. The author and J.N. wrote the first draft and finalized the paper together with other co-authors.

III **Studies on thermal atomic layer deposition (ALD) of silver thin films**

Maarit Mäkelä, Timo Hatanpää, Kenichiro Mizohata, Kristoffer Meinander, Jaakko Niinistö, Jyrki Räisänen, Mikko Ritala, Markku Leskelä
Chem. Mater. **29** (2017) 2040.
The author made the deposition experiments and performed the FESEM, EDS and GIXRD analyses and evaluated the electrical properties of the films. The author wrote the first draft and finalized the paper together with other co-authors.

IV **Thermal atomic layer deposition of continuous and highly conducting gold thin films**

Maarit Mäkelä, Timo Hatanpää, Kenichiro Mizohata, Jyrki Räisänen, Mikko Ritala, Markku Leskelä
Chem. Mater. **29** (2017) 6130.
The author made the deposition experiments and performed the FESEM, EDS and GIXRD analyses and evaluated the electrical properties. The author wrote the first draft and finalized the paper together with other co-authors.

V **Potential gold(I) precursors evaluated for atomic layer deposition**

Maarit Mäkelä, Timo Hatanpää, Mikko Ritala, Markku Leskelä, Kenichiro Mizohata, Kristoffer Meinander, Jyrki Räisänen
J. Vac. Sci. Technol. A. **35** (2017) 01B112.
The author made the deposition experiments and performed FESEM, EDS and GIXRD analyses and evaluated the electrical properties. The author wrote the first draft and finalized the paper together with other co-authors.

VI **Large-area plasmonic hot-spot arrays: sub-2 nm interparticle separations with plasma-enhanced atomic layer deposition of Ag on periodic arrays of Si nanopillars**

Joshua Caldwell, Orest Glembocki, Francisko Bezares, Maarit Kariniemi, Jaakko Niinistö, Timo Hatanpää, Ronald Rendell, Maraizu Ukaegbu, Mikko Ritala, Sharka Prokes, Charles Hosten, Markku Leskelä, Richard Kasica
Opt. Express **19** (2011) 26056.
The author did the deposition experiments of the Ag thin films and prepared the thiol SAM on the Ag surface. The author contributed in her part in writing the paper that was mostly written by J.C..

VII **Optimization of the silver nanoparticles PEALD process on the surface of 1-D titania coatings**

Aleksandra Radtke, Tomasz Jedrzejewski, Wieslaw Kozak, Beata Sadowska, Marzena Wieckowska-Szakiel, Ewa Talik, Maarit Mäkelä, Markku Leskelä, Piotr Piszczek
Nanomaterials **7** (2017) 193.
The author deposited the Ag coatings with A.R. The author contributed in her part in writing the paper that was mostly written by A.R..

The publications are referred to in the text by their roman numerals.

Abbreviations

ALD	atomic layer deposition
a.u.	arbitrary unit
btsa	bis(trimethylsilyl)amido
CVD	chemical vapor deposition
EDS	energy dispersive X-ray spectroscopy
FESEM	field emission scanning electron microscope
fod	(6,6,7,7,8,8,8-heptafluoro-2,2-dimethyl-3,5-octanedionato)
hfac	1,1,1,5,5-hexafluoroacetylacetonato
ICP	inductively coupled plasma
LIALD	liquid injection ALD
MHz	megahertz
OAc	acetate
PEALD	plasma-enhanced atomic layer deposition
Piv	pivalate, 2,2-dimethylpropionato
PVD	physical vapor deposition
REALD	radical enhanced atomic layer deposition
rf	radiofrequency
SAM	self-assembled monolayer
SERS	surface enhanced Raman spectroscopy
TGA	thermogravimetric analysis
thd	2,2,6,6-tetramethyl-3,5-heptanedionato
ToF-ERDA	time-of-flight elastic recoil detection analysis
XPS	X-ray photoelectron spectroscopy
XRD	X-ray diffraction
3D	three-dimensional

1 Introduction

This thesis is about atomic layer deposition (ALD) of Ag and Au thin films. A thin film consists of layers of atoms on a substrate surface.[1] Typical thicknesses of thin films are in the range of nano- and micrometers. ALD is a thin film deposition technique which relies on thermally stabile metal precursors. The metal precursor is evaporated and transported to the reaction chamber. It reacts with reactive groups on the surface in a self-limiting manner. One ALD cycle is finalized by supplying the other precursor, a co-reactant, to the chamber. Temperature of the deposition is a critical factor in an ALD process. The metal precursor should not decompose thermally in the gas phase or on the surface. The self-limiting growth is lost if the metal precursor decomposes. Still the temperature should be high enough to produce as pure thin films as possible with a high growth rate. Conformality is a unique feature of an ALD thin film. It means that the thin film follows the substrate surface exactly. Also in ALD, the film thickness can be precisely controlled in a nanometer level because of the self-limiting growth.[2-5] The basic concepts of ALD are introduced in Chapter 2.1. In the end of the Chapter, general requirements for a good ALD metal precursor are listed.

Plasma-enhanced atomic layer deposition (PEALD) is an energy enhanced version of thermal ALD.[5] One main advantage of PEALD is in general lower deposition temperatures as compared to thermal ALD. PEALD can accomplish processes at temperatures where the thermal reaction is not favored.[5] This is an important advantage especially with relatively unstable metal precursors. Considering the topic of this thesis, many ALD processes of Ag and Au are PEALD processes.[I,6-10] The major drawback of PEALD is stated to be the limited conformality of the thin films.[5] Literature surveys of PEALD and its advantages and drawbacks are introduced in Chapter 2.2.

Interest towards ALD of Au and Ag has risen during the last years. Potential applications are mostly in the field of photonics, electronics, catalysis and

biology.[11-13] In these applications substrates with complex structures are common and the required amounts of Ag and Au are small. ALD could enable conformal application of Ag and Au to these structures. With ALD the amount of the metal can be precisely controlled. Potential applications of Au and Ag thin films are briefly discussed in Chapter 2.3. The focus is kept on applications which were studied during this work.

In Chapter 2.4.1 general routes for depositing Ag and Au thin films by ALD are introduced as a background for the processes presented in Chapters 2.4.2 and 2.4.3. The existing Ag and Au processes can be categorized to thermal and plasma-enhanced ALD processes. Thermal Au processes can be further divided into processes where a true reducing agent has been applied or into combustion-type reactions where O_3 has been applied. In all thermal ALD processes of Ag, a reducing agent has been applied. However, there is no universal reducing agent for ALD and thus there is room for new reducing agents. In a general level, some selected reducing agents applied in ALD processes are presented in Chapter 2.4.1. Overall, ALD of Ag and Au thin films have been a challenge because of the low thermal stability of Ag and Au compounds. The silver compounds have often also low volatility.

The focus in this thesis was greatly on precursor chemistry and on finding more stable Ag and Au precursors for either thermal ALD or PEALD. In the experimental part (Chapter 4), the developed Ag and Au processes are presented and compared to literature. Chapter 4.1 focuses on Ag. One PEALD process of Ag was developed and the same Ag precursor was applied with a reducing agent in a thermal process to produce particulate Ag thin films.[I,III] In Chapter 4.2 a thermal ALD process of Au thin films by applying an Au(III) precursor and ozone is introduced.[IV] Also a chemical route for Au thin films by applying an Au(I) precursor and a reducing agent is discussed although this process was not self-limiting.[V] Properties of the deposited metal thin films are also presented. Crystallinity and microstructure of the thin films were characterized by X-ray diffraction (XRD) and field emission scanning electron microscope (FESEM). Electrical properties of the thin films deposited on an

insulator were evaluated with four-point probe measurements. Chemical composition of the Ag and Au thin films were analyzed by time-of-flight elastic recoil detection analysis (ToF-ERDA). More specific information of the processes and thin film properties are found in the publications.

Finally, in Chapter 4.3 two case studies of applying Ag to interesting applications are presented. In the first one, surface-enhanced Raman spectroscopy (SERS) substrates were coated with PEALD Ag. This led to significant improvements in Raman measurements.[VI] In the second study, titanium dioxide nanotubes and nanoneedles on titanium implants were coated with PEALD Ag. Antimicrobial activity was successfully gained.[VII] In the end Chapter 5 sums up the literature survey and the experimental work.

2 Background

2.1 Atomic layer deposition

ALD is a technique where a thin film is deposited in a heated ALD reactor typically in low pressure. In an ALD process two or more gaseous precursors are alternately fed into a reaction chamber. A term ALD cycle is used to describe the basic deposition unit of an ALD process. The first half-cycle starts when the first precursor, typically a vaporized metal precursor, is fed into the reaction chamber where the substrate is placed (Figure1(1a)). A typical substrate is a silicon wafer. Precursor molecules react with reactive surface groups of the substrate to form a layer which follows the texture of the surface. [2] Reaction byproducts and excess precursor molecules are purged away from the chamber after sufficient exposure time (Figure1(1b)). The second half-cycle starts when the other precursor, gaseous or vaporized co-reactant, is fed into the chamber. These molecules react with the reactive surface sites of the growing film to form a mono- or submonolayer of the desired thin film material (Figure1(2a)).[2] Again, after proper exposure time the excess co-reactant molecules and reaction byproducts are purged away (Figure 1(2b)). It is also possible that there are no reactive sites on the surface after the purge period (like in some metal ALD processes), still the growth of a thin film is possible through chemisorption. The metal precursor (or co-reactant) adsorbs on the surface and reacts during the next pulse with the other precursor.[14] The two half-cycles of an ALD cycle are repeated to increase the thin film thickness.[2]

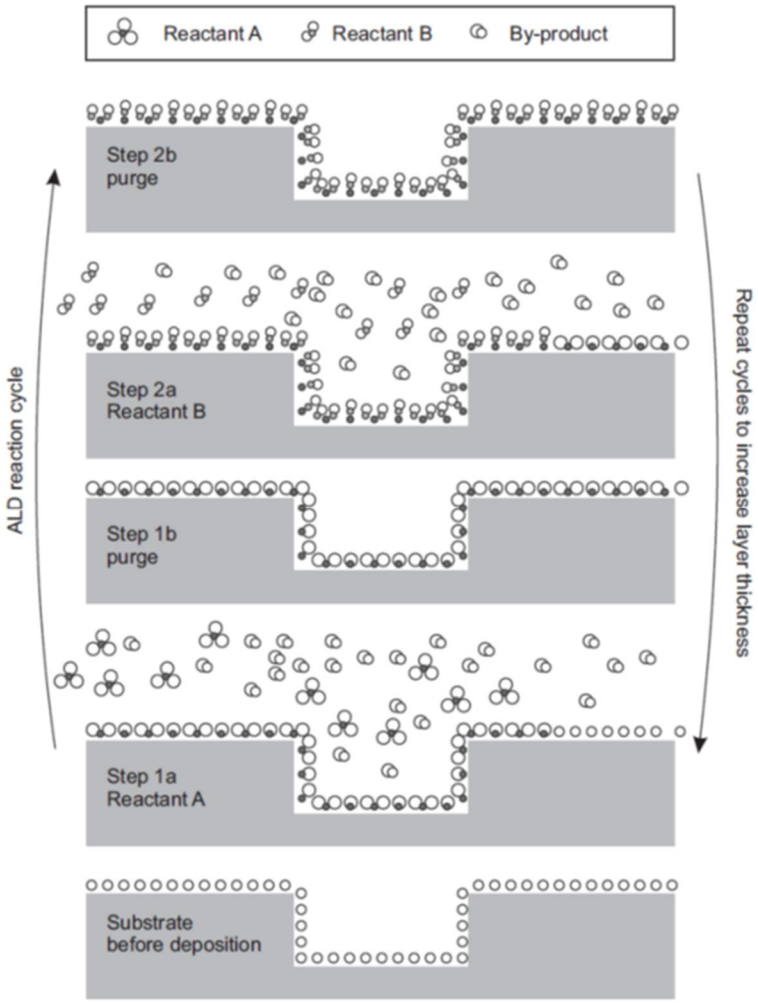

Figure 1. One ALD cycle divided to steps. The lowest image shows the substrate surface prior the deposition. The reactive groups are shown with circles. 1a) The metal precursor (Reactant A) is fed into the reaction chamber. 1b) Purge with an inert gas. 2a) The co-reactant (Reactant B) is fed into the reaction chamber. 2b) Purge with an inert gas. Reprinted from Journal of Applied Physics, vol. 113, pages 021301: 1-101, V. Miikkulainen et al.: "*Crystallinity of inorganic films grown by atomic layer deposition: Overview and general trends",* Copyright (2013), reproduced with permission from AIP Publishing LLC, http://aip.scitation.org/doi/citedby/10.1063/1.4757907

Typically, no complete monolayer of the thin film material is formed during one ALD cycle. This is prevented by steric hindrances between the ligands of the precursor molecules. Despite possible hindrances, ALD is still self-limiting meaning that the precursor molecules saturatively cover the surface.[2-5]

Deposition temperature plays a critical role in ALD. In general, five different temperature dependences can be considered when studying an ALD process

(Figure 2a). The most important temperature region is where the growth rate of the material is constant as a function of temperature (Figure 2a(1)). At these temperatures surface reactions are self-limiting and the film growth is ALD like. At lower temperatures reactions are not complete because of the limited reaction kinetics (Figure 2a(2)). The growth can still be self-limiting but the growth rate has not reached the saturated level. At low temperatures, it is also possible that the precursor molecules condensate physically and uncontrollably on the substrate if the deposition temperature is too low to keep the metal precursor in the gas phase (Figure 2a(3)). At temperatures above the ALD region, the precursor may decompose uncontrollably on the surface which results in higher growth rate than the saturated growth rate (Figure 2a(4)).[2-5] Alternatively, the growth rate may decrease if the precursor desorbs or a sticking constant of the precursor decreases (Figure 2a(5)).[15] When studying an ALD process, the effect of the deposition temperature to the growth is studied to find out the temperature limits of the self-limiting growth.[2-5]

The self-limiting ALD like growth is confirmed by changing the pulse length of a precursor at one specific deposition temperature. When the surface reactions are saturative, the growth rate of the film is constant as a function of the precursor pulse length (Figure 2b). Likewise, the purge length has no effect on the growth rate when the purge is long enough. If the growth rate increases as a function of the pulse length, the precursor decomposes thermally. It is also possible that the growth rate decreases with longer precursor pulses if the precursor or the reaction by-products are etching the film. In ALD the growth rate of the material is constant for every cycle because of the self-limiting growth. The film thickness increases linearly as a function of the cycles and the film thickness can be very precisely controlled by the number of the deposition cycles (Figure 2c).[2]

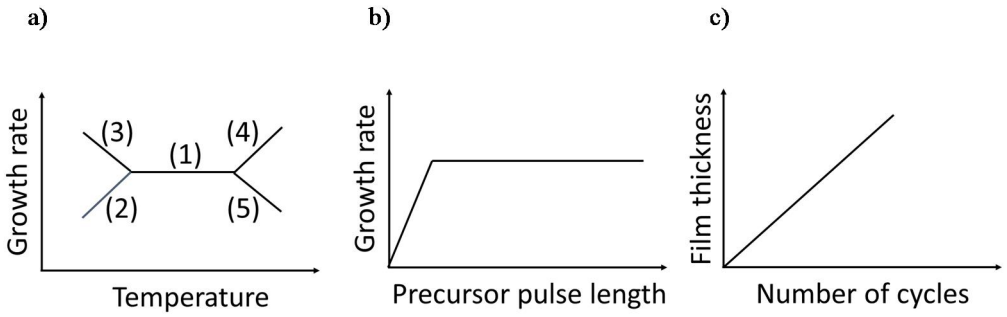

Figure 2. a) The possible temperature regions of an ALD process. 1) constant growth rate of the material as a function of temperature 2) temperature limits reactions 3) physical condensation 4) precursor decomposition and 5) desorption. b) Saturative growth of the material as a function of the precursor pulse length. c) Film thickness increases linearly as a function of the ALD cycles.

It has been noticed that when noble metal thin films are deposited by ALD by applying noble metal precursors and oxidizing agents, the growth rate may not stabilize as a function of the deposition temperature. This means that the growth rate increases as a function of the deposition temperature although the growth can be proven self-limiting by changing the precursors pulse lengths. This has been noticed e.g. in ALD processes of ruthenium thin films from bis(cyclopentadienyl)ruthenium and oxygen[16] and from tris(2,2,6,6-tetramethyl-3,5-heptanedionato)ruthenium and oxygen[17]. A constant growth rate as a function of the deposition temperature was neither noticed in a process where tris(2,4-pentanedionato)iridium and oxygen were applied to deposit iridium thin films.[18] These observations have been explained by active oxygen staying on the metal surface after the oxidizing agent pulse and the purge period. The active oxygen combusts part of the ligands of the metal precursor already during the metal precursor pulse.[14] The amount of active oxygen staying on the surface is dependent on temperature. Also in noble metal thin film ALD processes, the film thickness does not always increase linearly as a function of the cycles. Instead, a nucleation delay is often noticed in the beginning of a noble metal thin film growth.[19]

Binary materials are deposited by ALD by applying two precursors. Binary materials include many metal oxides, nitrides and sulphides. However, also ternary materials with three different kinds of ions, like $SrTiO_3$ and $BaTiO_3$, and elemental thin films,

metals and non-metals, can be deposited by ALD. Miikkulainen et al.[2] give a comprehensive list of the materials deposited by ALD.

The self-limiting surface reactions ensure the unique features of ALD thin films. The films are uniform in thickness over the substrate area. The films also cover the substrates conformally meaning that the films follow the structures of the substrates precisely. By ALD very complex three-dimensional, high aspect ratio substrates can be coated.[2-5] Other thin film techniques, and most of all, physical vapor deposition (PVD) techniques like sputtering and evaporation, do not produce as conformal thin films as ALD.[20] The most relevant limitation of ALD compared to other thin film deposition techniques is its slowness. Less than a monolayer of the desired material is deposited in one cycle. However, in many ALD applications very thin films are desired and slowness is therefore not that much of an issue.[3]

Industrial applications of ALD started from fabrication of electroluminescent (EL) displays.[21] Figure 3 shows an example of a multilayer stack prepared by ALD used in an EL display.[22] Outstanding industrial applications of ALD are in microelectronics where ALD is for instance used to deposit high quality thin films in the fabrication of memory components. These applications require pinhole free thin films with precise thickness control. Also, the device structures used in microelectronics are often very complex with high aspect ratios which ALD can coat conformally.[20,21] ALD thin films are also applied e.g. to photovoltaics and protective coatings.[20,23]

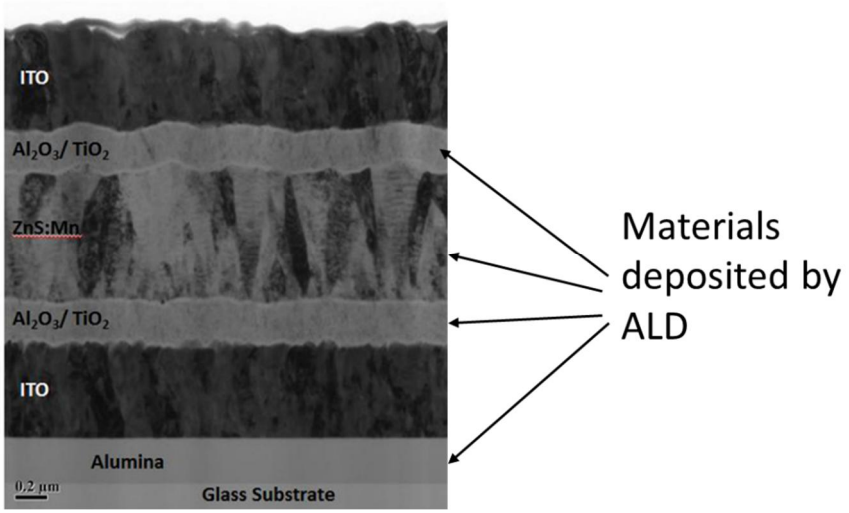

Figure 3. A cross sectional image of a multilayer stack used in an EL display. Materials deposited by ALD are marked. Image by Beneq Oy, ©Beneq.[22]

For a working ALD process it is essential to have good chemistry. The main requirements for a good ALD precursor are collected to Table 1. Firstly, the precursor must be volatile enough to ensure sufficient precursor flux to the reaction chamber. It is desirable that the metal precursor is a liquid or a low melting point solid compound. To ensure sufficient precursor flow to the reaction chamber, the precursor can be heated. It is also possible to use a bubbler source where carrier gas is mixed to a liquid precursor to raise the pressure in the source. Secondly the precursor should not self-decompose at the selected deposition temperature. Also, a good ALD metal precursor should endure continuous heating and pulsing. It has been estimated that the precursor should be stable up to 200 °C to be effectively used in ALD.[24] It is desirable that the precursor is highly reactive towards the surface groups. This ensures growth also at low deposition temperatures with complete reactions and produces pure thin films.[25] Low deposition temperatures (≤150 °C) are favored e.g. in production of metal thin films because the films deposited at lower temperatures are often smoother than the films deposited at higher temperatures.[24] High reactivity should be combined with high growth rate of the thin film. The high growth rate is secured by choosing precursors with ligands causing low steric hindrances. In addition to the above-mentioned criteria, a good ALD precursor is cheap, easy to use (easy to load into a reactor,

stabile in storage) and non-hazardous to the user and to the environment.[25] The last criteria involve also the precursor synthesis.

Table 1. General requirements for a good ALD precursor.

volatile (low evaporation temperature)
high thermal budget
reactive
cheap
easy to use (loading and storing)
non-hazardous (includes also precursor synthesis)

Often primary evaluation of thermal properties of a metal compound considered for ALD is carried out with thermogravimetric analysis (TGA). In TGA a small amount of the precursor is slowly heated under an inert atmosphere. The mass of the sample is weighed as a function of temperature and mass loss reveals the evaporation behavior of the compound. TGA shows whether the precursor evaporates without decomposition in a single step as desired from a good ALD precursor. From a TGA curve one can also evaluate proper evaporation temperature of the precursor inside an ALD reactor under reduced pressure.[26]

2.2 Plasma-enhanced atomic layer deposition

PEALD is an energy enhanced version of thermal ALD with the same operational principles as in thermal ALD. A PEALD cycle consists of pulses of a metal precursor and a co-reactant and purges in between with an inert gas. In PEALD the co-reactant is activated with plasma (Figure 4). A plasma source locates in the reaction chamber or very close to it. There is also a special modification of PEALD called radical enhanced atomic layer deposition (REALD). In a REALD reactor plasma is created further away from the chamber and only the reactive species of plasma are transported to the

reaction chamber.[6,27-31] Typical co-reactants in PEALD are gases (O_2 and H_2), but vapors like H_2O can also be applied.[5]

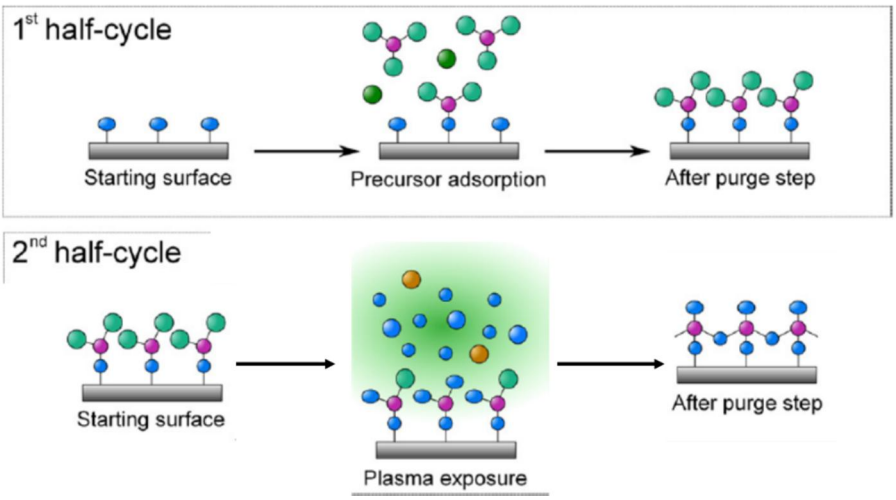

Figure 4. One PEALD cycle. During the 1st half-cycle the metal precursor is fed into the reaction chamber. During the 2nd half-cycle the co-reactant is activated with plasma. Figure modified from Journal of Vacuum Science and Technology A: Vacuum, Surfaces, and Films, vol. 29, pages 050801-26, H. B. Profijt et al.: *"Plasma-assisted atomic layer deposition: basics, opportunities, and challenges"*, Copyright (2011) with permission from AIP Publishing LLC. http://avs.scitation.org/doi/abs/10.1116/1.3609974

Plasma can be defined as ionized gas which consists of neutral molecules and atoms, ions (cations and anions) and electrons. Plasma can be fully or partially ionized.[32] When thin films are deposited by PEALD, plasma is formed using an electric field.[5] To be precise, in thin film manufacturing gas discharges are generated. PEALD plasma or a gas discharge is partially ionized and in non-thermal equilibrium meaning that temperatures of the plasma species are different from each other. This is because of the low pressure of the gas. In low pressure gases there are few collisions only in the plasma which results in different temperatures of the plasma species. Still, there can be localized areas where the temperatures of the plasma species are the same. In general, non-thermal equilibrium gas discharges are used in applications where heating is not wanted including etching and thin film deposition.[32]

In a PEALD process plasma is created by manipulating the free electrons of a gas by external electric field. The electrons of the gas collide inelastically with the gas atoms and molecules which results in excitation and ionization of the gas atoms and molecules. When the excited atom or molecule returns to its ground state, energy is released as radiation.[32] Excitation of the gas atoms and molecules results also in formation of radicals, which are very reactive atomic and molecular neutrals.[5] The radicals are the reactive species in the thin film growth in a PEALD process. Ionization of the gas atoms and molecules results in new electrons and ions. All the possible reactions in the plasma make the plasma self-sustaining.[32]

The two main types of plasma discharges used in PEALD reactors are capacitively coupled radiofrequency (rf) discharges and inductively coupled plasmas (ICP) (Figure 5). ICP is also created by applying rf currents (i.e. alternating voltages).[32] In the capacitively coupled rf discharge there are two electrodes in the reaction chamber where is also the plasma gas (like argon) and the substrate (Figure 5a). The plasma gas can be fed to the chamber from the side or through the top electrode with small holes making it a showerhead electrode. The other electrode is typically grounded, and the substrate is placed on the grounded electrode. It is also possible that between the top electrode and the grounded substrate holder there is a grounded grid (a mesh) which confines the plasma between the top electrode and the mesh.[5] ICP system is different from the capacitively coupled discharge. It is an electrodeless discharge. The plasma tube is surrounded by a coil where a rf current is running (Figure 5b). The rf current generates a rf magnetic flux in the coil which creates a rf electric field to the gas. The electric field accelerates free electrons of the gas and creates the plasma. Alternating electric field sustains the plasma.[32] The benefit of using the ICP system as shown in Figure 5b is that the plasma is generated far away from the substrate which makes optimization of the plasma easy and may also simplify process characterization e.g. temperature of the plasma is not changed when temperature of the substrate is varied when temperature ranges of an ALD precursor are studied.[5]

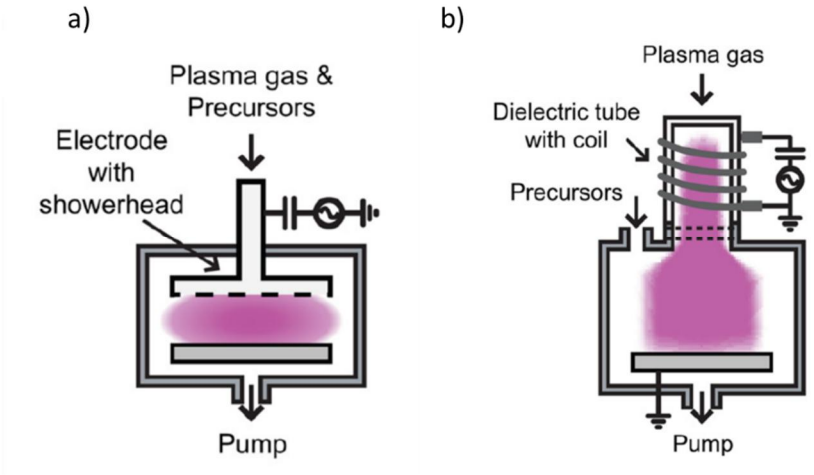

Figure 5. a) Schematics showing the reaction chamber with a capacitively coupled rf discharge system. The other electrode is grounded. b) Schematics showing the inductively coupled plasma (ICP) source. Images reprinted from Journal of Vacuum Science and Technology A: Vacuum, Surfaces, and Films, vol. 29, pages 050801-26, H. B. Profijt et al.: *"Plasma-assisted atomic layer deposition: basics, opportunities, and challenges"*, Copyright (2011) with permission from AIP Publishing LLC. http://avs.scitation.org/doi/abs/10.1116/1.3609974

In the alternating electric field, the electrons which are much lighter in mass compared to the heavy ions follow the alternating field. The ions, especially the heavy ones, are able to track only time-averaged electric fields.[32] This creates so called self-bias of the plasma. The voltage over the plasma has a positive value whereas the rf-powered electrode, if any, and all the other surfaces in the reaction chamber have a negative voltage.[32] The intrinsic self-bias of the plasma causes acceleration of positive ions towards the surfaces (including the substrate).[5]

In PEALD processes the degree of ionized particles compared to neutral species in the plasma is low. In general, the substrate faces mostly radicals. These radicals ensure thin film growth also at low temperatures where thermal reactions are kinetically limited. Only a small fraction of the electrons and ions reach the substrate. However, energy of the ions bombarding the substrate can be high because of the potential difference between the positive plasma and the negatively charged surfaces. In a PEALD process the energetic ions bombarding the surface can be beneficial by enhancing the surface reaction rates and e.g. surface diffusion. Because the substrate is typically grounded in

a PEALD process, the ion energies are often too small to cause damage but there are some examples of ion induced damage to the growing film.[5] For example degraded electrical properties were noticed in very thin HfO_2 thin films deposited by PEALD.[5,33,34]

The main types of gas discharges used in PEALD reactors were introduced above. One special notification should still be made. Beneq TFS 200 ALD reactor, used in this thesis work, is an ALD reactor with a capacitively coupled plasma source. In the reaction chamber there is a grid between the top electrode and the grounded substrate. The grounded grid confines the plasma between itself and the upper electrode. The hole size of the grid is critical: a diameter of a hole in the grid should be small enough to prevent electron and ion flow to the substrate.[35] Still the holes should be large enough to ensure sufficient and uniform radical flux to the substrate, if the reactive plasma gases are fed through the showerhead electrode to the reaction chamber. It is also possible to feed the reactive plasma gas from the side of the chamber to the substrates. The inert plasma gas like nitrogen or argon is still fed through the showerhead and plasma is ignited between the showerhead electrode and the grounded grid. The activation of the reactive plasma gas to radicals and other plasma species is possible because some amount of the reactive gas diffuses to the plasma region. Diffusion through the grid is possible because of pressure differences and prolonged exposure time. It is also possible in some cases that photoemission can activate the reactive plasma gas on the substrates.[36] This specific reactor can also be operated in a direct mode without the grid. Without the grid the flux of the ions to the substrate is larger.

As briefly mentioned above, in a PEALD reactor a gas discharge emits electromagnetic radiation because the accelerated electrons excite the gas atoms and molecules. The bound electrons of a gas atom are excited to higher electronic states. Molecules in turn are excited to higher electronic, vibrational and rotational states. When the excited electron returns to its ground state, energy is released by photon emission. Energies of the emitted photons are in the range of vacuum ultraviolet (100 – 200 nm) to visible (390 – 700

nm).[5,32] This radiation can be beneficial in the thin film deposition.[5] Actually, there is another energy enhanced version of ALD called photo-assisted ALD where the deposition is purely based on radiation. For instance, Lee *et al.*[37] reported self-limiting growth of ZrO_2 thin films by applying zirconium(tetra-tert-butoxide) ($Zr[OC(CH_3)_3]_4$) and water at room temperature (20 °C). During the water pulse the reaction chamber was irradiated by ultraviolet light. Without radiation, no growth was noticed. On the contrary it is also possible that plasma radiation causes damage to the thin film like in the study by Profijt et al.[38] who reported that vacuum ultraviolet radiation caused defect states to an Al_2O_3 thin film deposited by PEALD degrading the electrical properties of the film. The extent of the radiation induced damage could be affected by controlling the plasma pressure and the plasma power. When the pressure was higher, there was less damage and when the plasma power was higher, more damage was noticed.[38]

Materials deposited by PEALD have been reviewed by Profijt et al.[5] and include e.g. oxides, nitrides, carbides and metals. When industrial applications are considered, the 2012 Plasma Roadmap recognized PEALD as an interesting technique for depositing materials such as ZnO and TiO_2 at low temperatures for flexible devices.[39] Actually, a major advantage of PEALD compared to thermal ALD is in general lower deposition temperatures. The highest possible deposition temperature is often favored in thermal ALD processes to get the purest thin films. At low deposition temperatures in thermal ALD long purges are also often required to purge away excess precursor and co-reactant molecules from the reaction chamber. The polar water molecules are especially troublesome and time consuming to purge out at low temperatures in thermal ALD whereas in PEALD of oxides O_2 is much faster to purge out. PEALD thin films deposited at low temperatures can have equal properties as the corresponding thin films deposited by thermal ALD at higher temperatures because of the high reactivity of the radicals, extra-energy provided by the ions bombarding the surface, the recombination energy of the species at the surface and the plasma radiation.[5] By PEALD the temperature range of ALD processes can be widened to lower deposition temperatures if

the evaporation temperature of the metal precursor allows this and a proper plasma activated co-reactant is found.

In some cases, application of PEALD has resulted in higher growth rates compared to thermal ALD processes. It is assumed that plasma can create a higher density of reactive surface sites which leads to a high growth rate.[5] One advantage of PEALD especially at low deposition temperatures noted is that a PEALD cycle can be made shorter than the corresponding thermal ALD cycle which increases the productivity of a PEALD process. In PEALD the co-reactant can be in the reaction chamber at the same time as the metal precursor if they are not thermally reactive to each other at that specific deposition temperature. The purge after the plasma-activation can therefore be omitted to shorten the cycle time.[5]

The major drawback of PEALD is the limited conformality of the films. In thermal ALD conformality is limited only by diffusion of the precursor molecules from the main gas flow to the structures on the substrate. Long diffusion paths can be compensated by using long enough precursor pulses.[40] In PEALD in addition to precursor diffusion, radical recombination limits the growth. Close to a surface the radicals can either reflect from it or diffuse on the surface and recombine to non-reactive molecules.[5] Especially with polyatomic co-reactants (like NH_3) recombination can also take place in the gas phase.[27] In complex 3D structures the radicals collide with the surfaces several times before reaching the bottom of the structure. In general, recombination loss probability depends on the material. It is higher on metals than on oxides. Also, the co-reactants have different loss probabilities e.g. hydrogen radicals recombine more likely than nitrogen or oxygen radicals. [41] It is known that plasma parameters, such as plasma pulse length and plasma power, affect the conformality. Optimization of the processes is required. The plasma pulse length should be made long enough and plasma power high enough.[41,42] Also, when developing PEALD processes conformality of the thin film can be dependent on pressure and temperature in the reactor.[5,43] As a conclusion,

conformal thin films can be deposited by PEALD to complex structures with at least moderate aspect ratios.[5] There are also examples of conformal SiO_2 and HfO_2 thin films deposited by PEALD to very high aspect ratio structures by careful processes optimization. In this study the cylindrical trenches had an opening of about 115 nm and the height was about 6.75 µm resulting into an aspect ratio of 1:60.[II] As speculated in the paper, it is possible that a small secondary thermal ALD reaction pathway was present in these processes. Indeed, it has been proposed that a thermal pathway is always potentially present in a PEALD process when an oxide thin film is deposited from a metal organic precursor and oxygen radicals because of the water formed as a byproduct.[44] However, if the deposition temperature is low enough the thermal reaction pathway is not likely. The precursor should also be reactive with water. If the precursor is not reactive with water like the tris(dimethylamino)silane used for the SiO_2 deposition, formation of water should not result in thin film growth. It can still increase the amount of surface OH-groups which may have a role in the growth.[II] In addition, ozone is formed in oxygen plasma discharges through ion-neutral collisions.[45] It can improve conformality of the coating.

Another drawback of PEALD is that it is difficult to exploit in a batch mode. To gain sufficient growth rates and thin film uniformity, plasma should be generated close to the substrate and the whole substrate should face the radical source. To overcome this drawback, a specific PEALD type has been developed: spatial plasma-enhanced ALD. There are spatial plasma-enhanced ALD reactors where e.g. ten wafers can be coated at a time. Figure 6a shows the operating principle of one of the commercial spatial plasma-enhanced ALD reactors. The wafers rotate under the inlet of the metal precursor and the plasma zone. In between the precursor inlet and plasma zone there are zones of an inert gas. The number of rotations determines the film thickness.[46] There are also other kinds of spatial plasma-enhanced ALD reactors like the one where the substrate is moving linearly under the precursor feeding area and under the plasma discharge (Figure 6b).[47] The advantage of the spatial plasma-enhanced ALD compared to conventional PEALD is a high throughput

and a reduced cycle time because there is no need of purging the reaction chamber from the precursors.[7,46,47] Otherwise the advantages of spatial plasma-enhanced ALD are the same as the advantages of PEALD: the purge of the substrate after the plasma exposure can be shorter than after exposing the substrate to a co-reactant in a thermal ALD process (especially when comparing O_2 plasma and H_2O at low temperatures) and growth rates of the thin film materials can be higher compared to thermal ALD.[46]

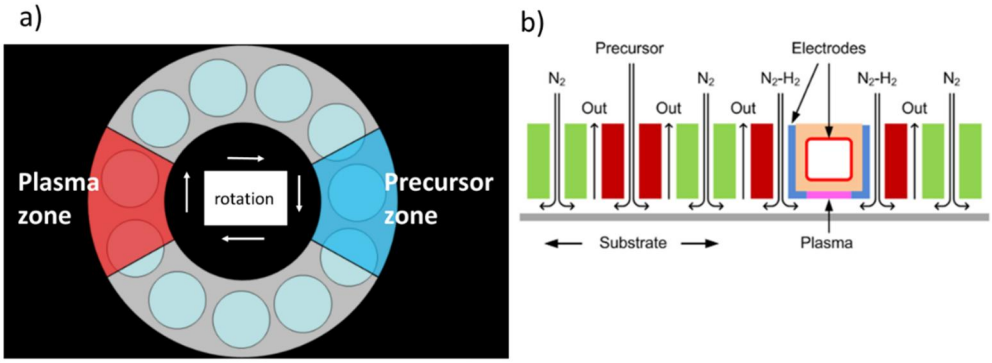

Figure 6. Schematic illustrations of spatial plasma-enhanced ALD reactors. a) rotary spatial plasma-enhanced ALD system b) linear spatial plasma-enhanced ALD system. a) Reprinted from IEEE Xplore Digital Library, S. Sneck et al.: *"Rotary Spatial Plasma Enhanced Atomic Layer Deposition- An enabling manufacturing technology for µm-thick ALD films"* ©2017 IEEE. http://ieeexplore.ieee.org/document/7919810/# b) Reprinted from Journal of Vacuum Science and Technology A: Vacuum, Surfaces, and Films, vol. 33. pages 01A131-(1-6), F. J. van der Bruele et al.: *"Atmospheric pressure plasma enhanced spatial ALD of silver".* Copyright (2015), reproduced with permission from AIP Publishing LLC. http://avs.scitation.org/doi/10.1116/1.4902561

2.3 Potential applications of silver and gold thin films deposited by ALD

During this thesis work, Ag thin films were deposited by PEALD for substrates designed for two applications, i.e. surface-enhanced Raman spectroscopy (SERS) and dental implants. Results from these experiments are presented in Chapter 4.3 while here these two applications are explained in more detail. Some other applications are also briefly mentioned.

Generally, Au and Ag are preferred materials in nanotechnology because of their high chemical and physical stability.[48] Both metals are highly

conducting. The bulk resistivity of Au is 2.44 μΩcm and that of Ag 1.59 μΩcm which is the lowest resistivity of all the elements.[49] High conductivity is desirable in electronics but is also the reason for the usage of these metals in photonics.[11] Photonics is a field of science where photons are controlled or manipulated in free space or in matter to gain new optics.[50] Ag and Au coatings can also be used in catalysis and in biological applications including e.g. biomedicine.[11,13,51] Because of the nature of these applications, it should be emphasized that although ALD often targets to continuous, pinhole free thin films, in the case of Ag and Au it can also be considered as an advantage that these metals grow first as islands in ALD. When the ALD growth starts the first nuclei appear on the substrate surface. When the growth proceeds, the first nuclei grow to nanoparticles while also new nuclei appear. After pulsing enough many cycles, the nanoparticles coalescence to larger islands which merge together and form a continuous thin film. Growth continues on the film. In the case of the noble metals, a nucleation delay is often noticed. This means that an effective nucleation starts only after tens or even hundreds of ALD cycles.[19] There are numerous ways to shorten the nucleation delay including use of precursors which have active adsorption properties toward the surface, feeding the metal precursor twice and using longer co-reactant pulses.[19] Hämäläinen et al.[19] gave a comprehensive report of nucleation in noble metal ALD.

For photonics Ag and Au are suitable materials because of their high conductivity and low refractive index in the visible wavelength region.[11,52] Free conduction band electrons of Ag and Au interact with an electric field of light and form either propagating surface plasmon polaritons in the case of continuous Ag or Au coatings, or localized surface plasmons in the case of metal nanoparticles.[11] A plasmon is defined as “a negatively charged electron cloud coherently displaced from its equilibrium position around a lattice made of positively charged ions”.[48] Figure 7 illustrates a simple case where light interacts with two spherical coinage metal (Cu, Au, Ag) nanoparticles.[12] The electric field of light is considered polarized and it is assumed that the electric field is uniform around the nanoparticle. The electric

field of light causes separation i.e. polarization of the charged particles of atoms. There is a net charge difference on the surface of the nanoparticle and this charge difference is the restoring force of the system. The restoring force tries to bring the system back to equilibrium and thus a dipolar oscillation of the free conduction electrons is created.[11,12,53] It should be highlighted that plasmons are created only in the depth of nanometers below the metal surface.[53] Another highlighted observation is that the electric field of the light at the surface is different from the electric field of the incoming light. When plasmons are created the electromagnetic fields are amplified.[12]

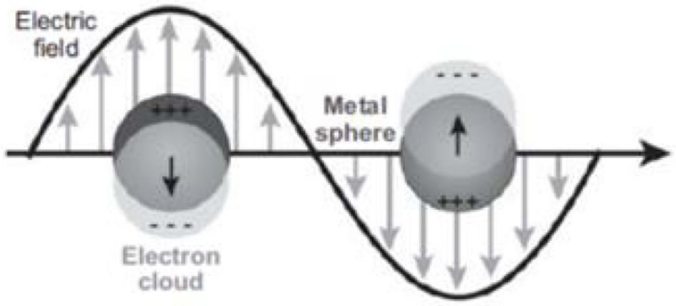

Figure 7. A scheme illustrating the interaction of the electric field of light with two coinage metal nanoparticles. Image reprinted from Annual Review of Analytical Chemistry, vol. 1, pages 601–626, P. L. Stiles et al. "*Surface-Enhanced Raman Spectroscopy*", Copyright (2008), reproduced with permission from Annual Reviews,
http://www.annualreviews.org/doi/full/10.1146/annurev.anchem.1.031207.112814

This interaction of light and nanoparticles is observed as color by eye. An example of this is a colloidal solution of spherical gold nanoparticles which has a red color.[11]

Surface-enhanced Raman spectroscopy (SERS) is a specific photonic application. It is a spectroscopy technique like conventional Raman spectroscopy and it is used to detect and identify chemicals. Extremely small quantities of molecules attached on a metal surface can be detected with SERS. The phenomenon exploited in SERS is called surface-enhanced Raman scattering (also abbreviated as SERS). Enhanced Raman scattering is noticed

for many specific molecules which are attached on a metal surface. The mechanism that produces enhanced Raman signals from the adsorbed molecules on the metal surface is a sum of many factors and includes an electromagnetic enhancement mechanism and a chemical enhancement mechanism. However, the basic idea is that the electric field of light excites surface plasmons on a rough metal surface. When there is a molecule attached on the surface, the electric field at the metal surface can induce an oscillating dipole in the molecule. This dipole can radiate light which is shifted by the vibrational frequency of the molecule.[12] By detecting these Raman scattered photons one gets information of the molecule attached on the surface. When the incident electric field and the scattered fields are resonant Raman scattering intensity is larger.[12] The largest enhancements are noticed for a metal surface which is rough on the nanoscale (10 – 100 nm).[55] Hence, SERS substrates are often designed to have e.g. needles and spherical shapes to maximize the Raman signal of the analyte molecules. It is also desired that the metallic nanostructures and nanoparticles are separated from each other by only nanoscale gaps. In the gaps, junction plasmons are created which effectively enhance the Raman signal of the analyte molecules.[55] Because of the complexity of the SERS substrates, ALD would be an ideal method to deposit either particulate or continuous Ag or Au thin films conformally on these substrates. Both metals are equally interesting for SERS but Ag shows the lowest losses of surface plasmons in the visible spectrum.[56] However, Ag is oxidized and reacts with sulfur compounds in air which is a concern.[57] Figure 8 shows an example of a Raman spectrum measured from a neat benzenethiol liquid compared to a normalized SERS spectrum measured from benzenethiol attached on a gold nanosphere monolayer. The intensity of the SERS spectrum is clearly higher than the Raman signal from the liquid.[58]

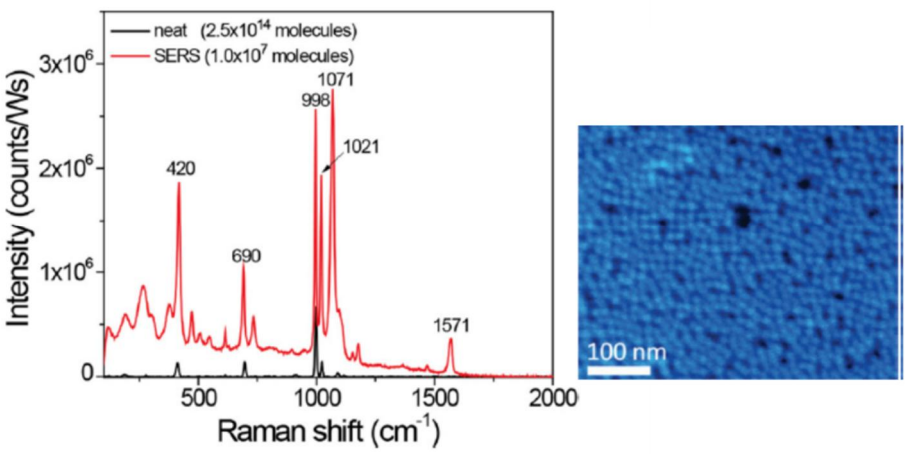

Figure 8. Left: Black line shows the Raman spectrum of a neat benzenethiol liquid. Red line shows the normalized SERS spectrum of a benzenethiol attached on an Au SERS substrate. Right: A SEM image of the Au SERS substrate consisting of a monolayer of spherical Au nanoparticles. Reprinted from Applied Physics Letters, vol. 102, pages 201606(-1-6), J. Fontana et al.: *"Large surface-enhanced Raman scattering from self-assembled gold nanosphere monolayers"*, Copyright (2013), reproduced with permission from AIP Publishing LLC. http://aip.scitation.org/doi/full/10.1063/1.4807659

For medical applications, Ag is considered as an excellent biomaterial because it has low toxicological effect on human body. In these applications an antimicrobial effect of Ag is pursued.[59,60] The antimicrobial effect is based on the release of Ag^+ ions. Silver ions bind to the S, O or N containing biological groups of the foreign biomaterial.[59,61] However, Ag^+ ions bind also to other chemical species containing S, Cl, O, C or N occurring naturally in the body and form products such as Ag_2S which are toxic to cells.[59,62] Thus, the release of Ag^+ ions should be controlled in the biomaterial.[59] Examples of Ag biomaterials are wound dressings[59,63] and filling materials for dental applications.[59,64]

2.4 Atomic layer deposition processes of silver and gold thin films

Ag and Au thin films have been deposited either by thermal ALD or PEALD. In total, there are only ten processes for Ag and three for Au thin films. Two of the Ag and two of the Au processes were developed in this thesis work. The following chapters focus in precursor properties instead of the thin film properties. Mainly thermal properties of the Ag and Au precursors are compared. In the experimental part (Chapter 4) the results of the developed Ag and Au processes are discussed in detail and compared with the literature.

2.4.1 Possible pathways to atomic layer deposition of silver and gold thin films

The existing ALD processes of Ag and Au can be categorized to thermal and PEALD processes. The thermal ALD processes can be further categorized to processes where a reducing agent has been applied, and in case of Au, also to processes which are called combustion-type processes. These combustion-type processes are common in noble metal ALD and rely on that the corresponding oxides are not stable at the deposition temperatures.[14] In the noble metal processes of Ru, Os, Rh, Ir and Pt thin films, the metal precursors have been applied with O_2 at temperatures above 200 °C. At lower temperatures Ru, Rh, Ir and Pt oxides have been deposited with O_3.[19] Metal precursors like $RuCp_2$, $MeCpPtMe_3$, $Ru(thd)_3$ and $Ir(acac)_3$ which are thermally very stable have been used in the combustion-type processes.[16-18,65] Au thin films can also be deposited by combustion reaction by applying an oxygen source with a thermally stabile Au precursor. 170 °C is the temperature where Au_2O_3 is expected to decompose to a possible Au_2O intermediate and further to Au.[66] However, in an ALD process decomposition can happen already at lower temperatures because the chemical potential of a deposited monolayer is higher than the chemical

potential of bulk material.[10] The oxide can also react with the organic ligands of the metal precursor. The mechanism of the growth in the combustion-type noble metal ALD processes has been studied.[14] It is still unclear, however, how the growth starts on an oxide surface. It has been speculated that the precursor must slightly decompose to initiate the growth.[2] In practice combustion-type processes are easily carried out, because the most evident reactants being O_2 and O_3 are gases and routinely used in ALD processes.

Application of a true reducing agent to an ALD process is another option to obtain Ag and Au thin films. Requirements for a good reducing agent are the same as for a metal precursor listed in Chapter 2.1. The most relevant are that the reducing agent does not decompose to non-volatile species and forms volatile byproducts with the ligands of the metal precursor. The reducing agent should not leave impurities to the film, e.g. oxygen containing reducing agents are not good choices for transition metal processes because of the high probability of transition metal oxide formation. To date there are not that many ALD processes with true reducing agents.[2] However, the number of processes is increasing. Some examples of the reducing agents used in the ALD processes are briefly discussed here.

Another noble metal thin films, Pd thin films, have been deposited by applying reducing agents including H_2, formalin and glyoxylic acid.[19,67-71] In general, reducing gases are easily delivered to the reaction chamber but safety issues with e.g. H_2, Si_2H_6 and B_2H_6 are important to consider. Si_2H_6 and B_2H_6 are pyrophoric gases.[72,73] Molecular H_2 is often not reactive enough to reduce the metal precursors at least at low deposition temperatures. Hydrides containing e.g. B-H, Al-H or Si-H bonds can transfer hydrogen to a metal center resulting in metal hydrides which are unstable. H_2 is eliminated and metal center is reduced.[24] Recently, new selective reducing agents have been introduced. 2-methyl-1,4-bis(trimethylsilyl)-2,5-cyclohexadiene and 1,4-bis(trimethylsilyl)-1,4-dihydropyrazine were applied with $TiCl_4$ to deposit Ti thin films.[74] The reaction was most likely based on an interaction of

electron-deficient Ti and electron-rich cyclic ring.[74,75] Also a formation of trimethylsilyl chloride as a byproduct could be a driving force in the reaction.[74] Another example of the reduction selectivity are transition metal processes based on $BH_3(NHMe_2)$.[76,77] In these metal processes for Cu, Ni, Co, Fe, Mn and Cr thin films the reduction took place only on a catalytic Ru surface, that most likely converted $BH_3(NHMe_2)$ to more reducing species. Even on the catalytic substrate, a nucleation period was required to get the growth started. The nucleation period resembled normal ALD cycling (50 cycles of 20 s pulse of a metal precursor, 5 s purge, 1 s pulse of $BH_3(NHMe_2)$ and 10 s purge). The processes wherein $BH_3(NHMe_2)$ has been applied show that partial decomposition of a precursor is not always detrimental to ALD. Saturation of the growth rate of the metal as a function of $BH_3(NHMe_2)$ was shown.[76,77] Reduction selectivity in respect to the substrate can be beneficial in some applications where selective ALD is looked for.

2.4.2 Silver ALD processes

Overlooks of the PEALD and thermal ALD processes of Ag are collected to Tables 2 and 3. Among the PEALD processes there is also a spatial plasma-enhanced ALD processes. This technique was in more detail introduced in the end of Chapter 2.2 (Plasma Enhanced Atomic Layer Deposition). Thermal ALD processes include also liquid injection ALD (LIALD) processes where the metal precursor is dissolved to a solution to assist vaporization of the precursor. Lower evaporation temperature can accomplish depositions at lower temperatures which can be beneficial with thermally relatively unstable metal precursors.[78] Schematics of the Ag precursors mentioned in Tables are shown in Figure 9.

Table 2. PEALD processes of Ag thin films. The spatial plasma-enhanced ALD processes are highlighted with a grey color.

Ag precursor	**source temperature of the Ag precursor (°C)**	**reducing agent**	**ALD window (°C)**	**growth rate**	**ref.**
$Ag(O_2C^tBu)(PEt_3)$	125	H_2/Ar	140	1.2 Å/cycle	[6]
$Ag(O_2C^tBu)(PBu_3)$		H_2/Ar			[6]
$Ag(fod)(PEt_3)$	106	H_2/Ar	120 – 140	0.3 Å/cycle (0.15 nm/min)	I
$Ag(fod)(PEt_3)$	100, 120	H_2/N_2	depositions at 100, 120	0.8 nm/min	[7]
$Ag(fod)(PEt_3)$	110	H_2/Ar	depositions at 70, 120, 200	0.3 Å/cycle	[8]
$Ag(fod)(PEt_3)$	95	NH_3	130	2.4 Å/cycle	[9]
$Ag(fod)(PEt_3)$	95	H_2	130	0.4 Å/cycle	[9]

Table 3. Thermal ALD processes of Ag thin films. LIALD processes are highlighted with a grey color.

Ag precursor	**source temperature of the Ag precursor (°C)**	**reducing agent**	**source temperature of the reducing agent (°C)**	**ALD window (°C)**	**growth rate (Å/ cycle)**	**ref.**
Ag(hfac)(1,5-COD) (dissolved in toluene)	50	propan-1-ol	RT**	110–150		[79]
Ag(hfac)(1,5-COD) (dissolved in toluene)	130*	propan-1-ol	20	123–128	0.16	[80]
Ag(hfac)(1,5-COD) (dissolved in toluene)	130	$tBuHNNH_2$	20	105–128	0.18	[81]
Ag(hfac)(PMe_3)	~63 – 66	formalin (i.e. formaldehyde, 37 w % in H_2O with 10 % methanol in H_2O)	RT**	at 200	0.07 (2 – 10 ng/cm^2 / cycle)	[82]
Ag(hfac)(PMe_3)	~63 – 66	$AlMe_3$ and H_2O	RT**	170 – 200	1 – 2 ng/cm^2 /cycle	[82]
Ag(fod)(PEt_3)	95	BH_{3-} ($NHMe_2$)	32	110	0.33	III

*carrier flow through the source enhanced vaporization, **RT = room temperature

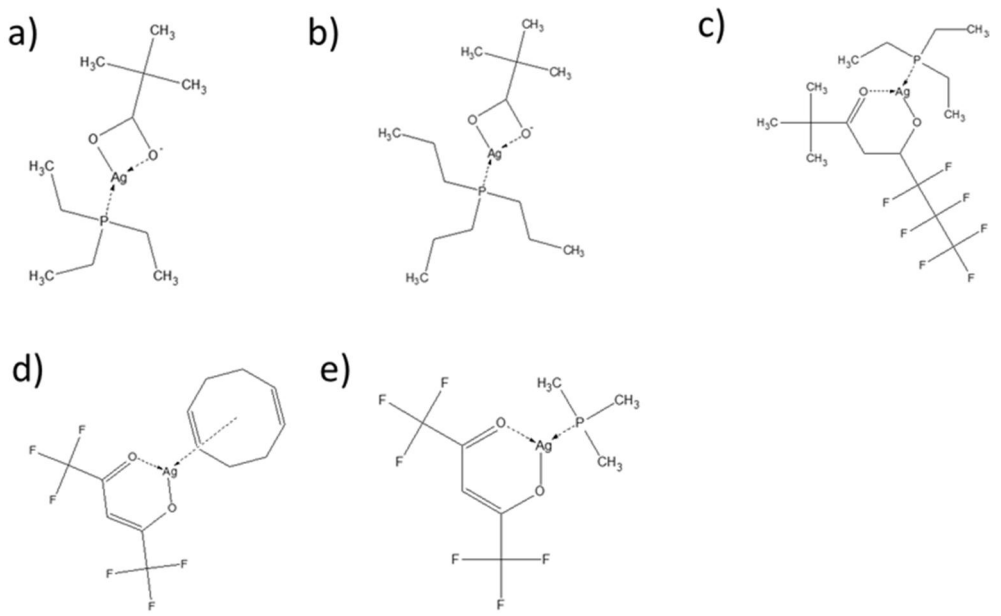

Figure 9. Schematics of the Ag precursors listed in Tables 2 and 3 showing the existing ALD processes of Ag thin films. a) Ag(O_2C^tBu)(PEt_3), b) Ag(O_2C^tBu)(PBu_3), c) Ag(fod)(PEt_3), d) Ag(hfac)(1,5-COD), e) Ag(hfac)(PMe_3).

The first Ag study was a REALD process introduced by Niskanen et al.[6] (2,2-dimethylpropionato)silver(I)triethylphosphine (Ag(O_2C^tBu)(PEt_3)) was used with plasma activated hydrogen. Ag(O_2C^tBu)(PEt_3) showed good ALD characteristics with a high growth rate of 1.2 Å/cycle. However, the evaporation temperature of Ag(O_2C^tBu)(PEt_3) was 125 °C and the decomposition temperature around 160 °C making the ALD temperature range narrow. In the same study (2,2-dimethylpropionato)silver(I)tributylphosphine (Ag(O_2C^tBu)(PBu_3)) was briefly studied, but no process could be reported.

(Hexafluoroacetylacetonato)silver(I)(1,5-cyclooctadiene) (Ag(hfac)(1,5-COD)) has been used in three LIALD studies.[79-81] Application of propan-1-ol as a co-reactant showed a narrow ALD window at 123 – 128 °C.[80] The ALD window was widened to lower temperatures by applying a more reactive co-reactant: tert-butylhydrazine ($tBuHNNH_2$).[81] By applying $tBuHNNH_2$, the ALD growth was achieved at deposition temperatures of 105 – 128 °C. Growth rate of Ag was nearly the same with both co-reactants (0.16 and 0.18

Å/cycle), which shows that the adsorption density of Ag(hfac)(1,5-COD) is mostly determining the growth rate on Si. A clear difference in the results of these studies was that application of propan-1-ol resulted in particulate Ag coatings with high texture whereas application of $tBuHNNH_2$ resulted in much smoother Ag thin films on Si. The differences in the thin film textures were explained with different growth mechanisms. When propan-1-ol was used as a reducing agent, the reduction reaction of chemisorbed Ag(hfac)(1,5-COD) was believed to take place only on Ag surface whereas $tBuHNNH_2$ was supposed to be reactive with the chemisorbed Ag(hfac)(1,5-COD) also directly on Si.[81] It can be speculated that minor decomposition of Ag(hfac)(1,5-COD) is required to make propan-1-ol to work as a reducing agent in this process. The achieved growth rates of Ag (0.16 and 0.18 Å/cycle) are clearly lower than the growth rate of Ag in the REALD process with $Ag(O_2C^tBu)(PBu_3)$ and plasma activated hydrogen (1.2 Å/cycle). [6,80,81] The low growth rate is most likely a result of large ligands causing steric hindrances.

Triethylphosphine(6,6,7,7,8,8,8-heptafluoro-2,2-dimethyl-3,5-octanedionato)silver(I) ($Ag(fod)(PEt_3)$) has been used both in PEALD processes with plasma activated H_2 and NH_3 and in a thermal process with $BH_3(NHMe_2)$.[I,III,7-9] $Ag(fod)(PEt_3)$ starts to decompose around 120 – 140 °C depending on the reactor type. Again, the ALD temperature range is narrow because the evaporation temperature of $Ag(fod)(PEt_3)$ has been 91 – 106 °C.[I,III] Growth rates of Ag achieved within the ALD regime were 0.3 – 0.4 Å/cycle on Si when either plasma-activated H_2 or $BH_3(NHMe_2)$ were applied.[I,III,9] However, with plasma-activated NH_3 the growth rate of Ag was significantly higher, 2.4 Å/cycle.[9] It is likely that the growth of Ag is always restricted by the steric hindrances of relatively large ligands of $Ag(fod)(PEt_3)$.[I,III,9] The difference in the growth rates of Ag in the processes was explained with the different reactive groups of the surface after the plasma exposure. It was believed that after the NH_3 plasma exposure the Ag surface was saturated with stable and reactive NH_x surface groups. When the surface was again exposed to $Ag(fod)(PEt_3)$, the first $Ag(fod)(PEt_3)$ molecules reacted with the NH_x surface groups losing their ligands and after these reactions were

completed further Ag(fod)(PEt_3) molecules could still chemisorb on the surface. By contrast, after the H_2 plasma exposure the surface was believed to be saturated with Ag-H surface groups which are not stable. When the surface was again exposed to Ag(fod)(PEt_3), it only chemisorbed to the Ag(0) surface. This difference in reaction of Ag(fod)(PEt_3) with the surface resulted in different growth rates. It should be mentioned that without plasma activation NH_3 gas was not able to reduce chemisorbed Ag(fod)(PEt_3) at the studied temperature.[9]

(Hexafluoroacetylacetonato)silver(I)trimethylphosphine (Ag(hfac)(PMe_3)) has also been studied for ALD of Ag.[82] Two processes were tested to coat silica gel samples. In the first process Ag(hfac)(PMe_3) was applied with formalin. The growth rate was low, 0.07 Å/cycle, at 200 °C. In the other process Ag(hfac)(PMe_3) was applied with trimethylaluminium and water. This process produced Ag coatings already at 110 °C but the growth rate was even lower, only ½ or 1/10 of that with formalin.[82]

As a conclusion, all the Ag precursors are thermally quite unstable and ALD temperature ranges are very narrow. The decomposition temperatures reported for the Ag precursors are 170 °C for Ag(O_2C^tBu)(PEt_3), 128 °C for Ag(hfac)(1,5-COD), 140 °C for Ag(fod)(PEt_3), and around 200 °C for Ag(hfac)(PMe_3). These are low temperatures for ALD precursors. The large ligands make the precursors heavy and evaporation temperatures high which is not beneficial in ALD. Ag(fod)(PEt_3) and Ag(hfac)(1,5-COD) have ligands that contain fluorine to make the precursors more volatile. Fluorine has also strong electron affinity which stabilizes the precursor. The neutral tertiary phosphine ligands in Ag(fod)(PEt_3), Ag(O_2C^tBu)(PEt_3) and Ag(hfac)(PMe_3) are supposed to stabilize the precursor through π bonding.[83] In general, neutral ligands like phosphines are not preferred choices to ALD precursors because the dissociation of the neutral ligand provides a decomposition pathway to less volatile metal complexes already at low temperatures.[24] Clearly the challenge with Ag has been in finding enough volatile and thermally stabile Ag precursor for ALD.

2.4.3 Gold ALD processes

The existing processes for Au thin films are collected to Table 4. The last process is not entirely true ALD process because no self-limiting growth was confirmed. However, the process still produced pure Au thin films when a metal precursor and a co-reactant were pulsed alternately in an ALD process manner. This process is relevant to mention here because several Au(I) precursors were evaluated for ALD in the paper. Schematics of the Au precursors of Table 4 are shown in Figure 10.

Table 4. ALD processes of Au thin films. The PEALD process is highlighted with a grey color.

Au precursor	source temperature of the Au precursor (°C)	reducing agent	ALD growth confirmed (°C)	growth rate (Å/cycle)	ref.
$Me_3Au(PMe_3)$	85	O_2 plasma and H_2O	120	0.5	[10]
$Me_2Au(S_2CNEt_2)$	99	O_3	180	0.9	[IV]
$Au(N(SiMe_3)_2)(PEt_3)$	61	$BH_3(NHMe_2)$			[V]

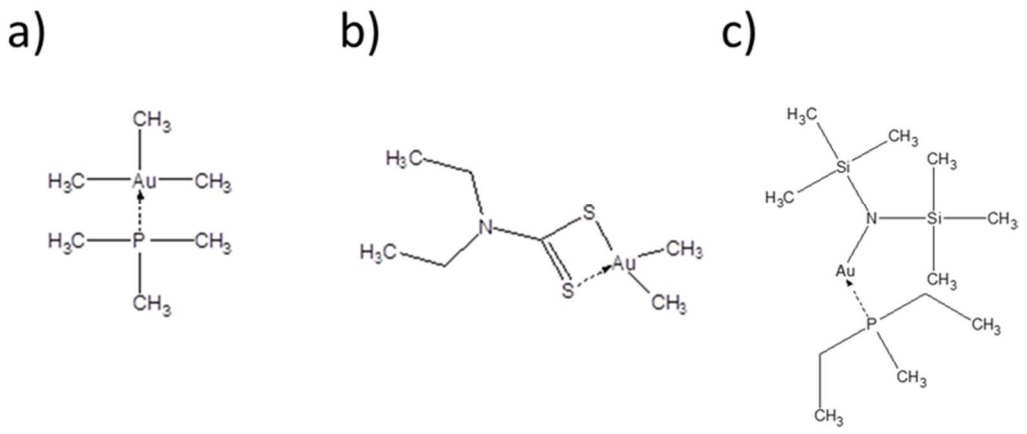

Figure 10. Schematics of the Au precursors listed to Table 4 showing the existing Au processes of the Au thin films. a) $Me_3Au(PMe_3)$ b) $Me_2Au(S_2CNEt_2)$ c) $Au(N(SiMe_3)_2)(PEt_3)$

The first Au process was a PEALD process where trimethylphosphinetrimethylgold(III) ($Me_3Au(PMe_3)$) was applied with plasma-activated oxygen and water.[10] Au thin films were obtained at 120 °C and the process showed self-limiting growth when the $Me_3Au(PMe_3)$ pulse length was varied. Thermal route to Au thin films by using either O_3, H_2O or molecular O_2 was also tried but no growth was obtained. Application of water after the O_2 pulse was crucial to obtain high quality Au thin films. When water was not applied the process produced discolored films with excessive amounts of impurities. The impurities were attributed to be a result of trimethylphosphine reacting with oxygen to phosphorous(V) oxide. When a water pulse was added to the cycle, hydrolysis of the phosphorous oxide impurities to phosphorous acid happened. Phosphorous acid is volatile at the studied growth temperatures. In general, $Me_3Au(PMe_3)$ was concluded to be a liquid precursor with great volatility and sufficient thermal stability. Thermal decomposition was observed at 130 °C.[10]

The first thermal ALD process of gold was developed during this thesis work. In the process, continuous and conductive Au thin films were deposited by applying dimethylgold(III)diethyldithiocarbamato ($Me_2Au(S_2CNEt_2)$) and O_3. $Me_2Au(S_2CNEt_2)$ seemed to be an excellent ALD precursor. It is a solid but melted to liquid at the evaporation temperature used. It clearly decomposed only at 250 °C. Au thin films were deposited at 120 – 200 °C and self-limiting growth was confirmed at 180 °C with a growth rate of 0.9 Å/cycle. The main issue of $Me_2Au(S_2CNEt_2)$ was the low synthesis yield. The overall yield of the synthesis was only 10 % although the literature yield was expected to be over 50 %.[III,84,85]

Seven Au(I) compounds were evaluated for ALD of gold thin films.[V] (Bis(trimethylsilyl)amido)(triethylphosphine)gold(I) ($Au(N(SiMe_3)_2)(PEt_3)$) was chosen for the deposition experiments based on the evaluation of the thermal properties of the compounds. It was pulsed alternately with $BH_3(NHMe_2)$ to deposit Au thin films. Severe decomposition was noticed only at 160 °C but no self-limiting growth was confirmed either at lower deposition

temperatures. Growth rate of Au was very low, only 0.05 – 0.06 Å/cycle at 80 – 140 °C. At 100 °C the growth rate was noticed to decrease when more cycles were applied i.e. when the film was supposed to grow on itself instead of a Si surface. The reason for this remained unclear but it was proposed that PEt_3 passivated the Au surface after some Au metal had been deposited.[V]

Overall, the two Au(III) precursor were found thermally more stabile than any of the Au(I) compounds studied. Thermally the most stabile Au precursor was $Me_2Au(S_2CNEt_2)$. Both $Me_3Au(PMe_3)$ and $Au(N(SiMe_3)_2)(PEt_3)$ contained a phosphine ligand which can stabilize the precursor through π-bonding but can provide a decomposition pathway to less volatile metal complexes already at low temperatures.[24,83] In both processes the phosphine ligand was speculated to remain on the Au surface and cause passivation of the surface or phosphine impurities to the Au thin films.[V,10]

3 EXPERIMENTAL

In this chapter, the experimental details of the thin film deposition and characterization are described. The detailed information of the processes can be found from the publications I-VII. Also, information of the precursor synthesis and characterization are presented in the publications. Here are shown only the results from thermogravimetric analysis which were used to evaluate thermal and evaporation properties of the precursors.

3.1 Precursor characterization

Thermal properties of the synthesized precursors were evaluated by performing thermogravimetric analysis using a Mettler Toledo Star^e system equipped with TGA850 thermobalance. The measurements were done at atmospheric pressure using N_2 as the purge gas. Heating rate was 10 °C/min and the sample size was 10 – 11 mg. Melting point was taken from the single differential thermal analysis (SDTA) data measured by the thermobalance.[I,III,IV,V]

3.2 Thin film deposition

The PEALD process of Ag thin films was developed in a Beneq TFS 200 ALD reactor. It is a cross-flow reactor which can be operated in both thermal and plasma-enhanced ALD modes. In these studies, only the plasma mode was used. Ag(fod)(PEt_3) was loaded to an open boat and inserted to a hot source. Evaporation temperature was 106 °C. A carrier gas was Ar (AGA, 99.999 %) and plasma-activated H_2 (AGA, 99.999 %) was used as a reducing agent. Both Ar and H_2 were purified on site with Aeronex GateKeeper and Entergris Gatekeeper purifiers. The plasma discharge was generated by capacitive coupling with a 13.56 MHz rf power source. The reactor had a remote configuration where a metallic mesh (a grid) was placed between the rf

coupled upper electrode and the wafer holder (Figure 11).[I] Plasma power was typically 100 W. Ag thin films were deposited on Si(100) and glass substrates. The pressure in the reactor during the depositions was 5 – 10 mbar. To study the conformality of the PEALD Ag thin films, Ag was deposited on 3D structures consisting of cylindrical trenches whose height was about 6.75 µm and opening about 115 nm leading to an aspect ratio of about 60:1. In this deposition the Ag(fod)(PEt_3) pulse length was 5 s and the hydrogen plasma exposure time was 7 s.[II]

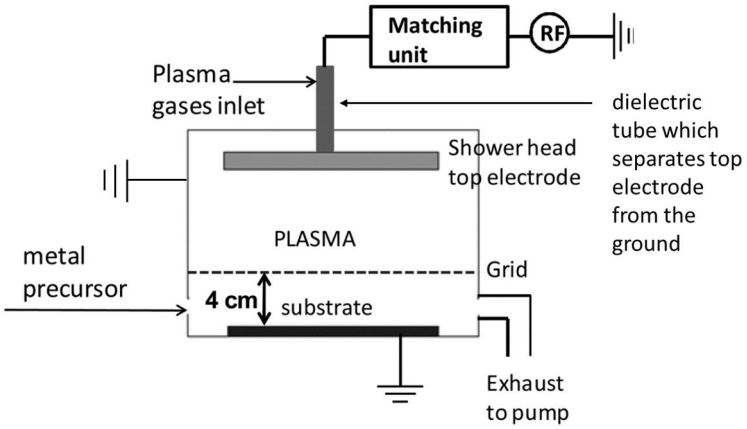

Figure 11. Schematic illustration of the reaction chamber in a Beneq TFS 200 ALD reactor. Image modified from Chemistry of Materials, vol. 23, pages 2901-2907, M. Kariniemi et al.: *"Plasma-Enhanced Atomic Layer Deposition of Silver Thin Films"*, Copyright (2011), reproduced with permission from American Chemical Society. http://pubs.acs.org/doi/10.1021/cm200402j

SERS substrates and titanium implants with titanium dioxide nanotubes and nanoneedles on top were coated with PEALD Ag as described above. On the SERS substrates a thiophenol monolayer was prepared right after the Ag deposition and then used as the analyte molecule in the Raman spectroscopy.

Au and Ag thin films were deposited by thermal ALD in an ASM Microchemistry F120 ALD reactor which is a cross-flow cassette reactor and relies on inert gas valving.[86] The inert gas in the reactor was N_2 (AGA, 99.999 %). Two 5x5 cm^2 substrates, usually Si(100) and glass, were inserted to a reaction chamber. In some experiments, also catalytic substrates like Ru were used. Pressure in the reactor was 5 – 10 mbar during depositions. All the

metal precursors and solid co-reactants were loaded to glass boats either in a fume hood or in a glove box and inserted to the reactor. The metal precursors and co-reactants studied are listed in Table 5. One of the co-reactants considered as a potential reducing agent, Et_3SiH is a high vapor pressure liquid and it was supplied from an external source. Gases, O_2 (AGA, 99.999 %) and H_2 (AGA, 99.999 %) were also used. Ozone was produced from O_2 using an O_3 generator (Wedeco Ozomatic Modular 4 HC Lab). The O_3 concentration was about 100 g/Nm^3, and the total flow rate of O_2/O_3 mixture was set to ~75 sccm with a needle valve. In the experiments where H_2S was used the flow rate of H_2S was about 6 sccm. In some experiments, catalytic material being pieces of sputtered Ru on a Si wafer was inserted to the reactor. This was done to activate $BH_3(NHMe_2)$ which was used as a reducing agent. In these experiments Ru was inserted to the source tube of $BH_3(NHMe_2)$ so that only $BH_3(NHMe_2)$ was in contact with Ru before reaching the reaction chamber and the substrates.

Table 5: The studied metal precursors and co-reactants which are highlighted with a grey color. F120 refers to the ASM Microchemistry F120 ALD reactor and TFS 200 to the Beneq TFS 200 ALD reactor.

Compound	**Evaporation temperature (°C)**	**Origin of the compound**
$Ag(fod)(PEt_3)$	F120: 95	Strem Chemicals, Inc.
	TFS 200: 106	Home synthesized
$Me_2Au(S_2CNEt_2)$	F120: 99	Home synthesized
$Au(N(SiMe_3)_2)(PEt_3)$	F120: 61	Home synthesized
$BH_3(NHMe_2)$	F120: 32	Sigma-Aldrich
$BH_3(NMe_3)$	F120: 20	Sigma-Aldrich
$C_6H_6O_2$ (benzene-1,4-diol, hydroquinone)	F120: 118	Sigma-Aldrich
Et_3SiH	F120: 22	Sigma-Aldrich (99 %)
H_2S		Aldrich (99.5 %)

3.3 Thin film characterization

Thicknesses of the Ag and Au thin films deposited on Si(100) were measured with energy dispersive X-ray spectroscopy (EDS) (Oxford INCA 350 Energy spectrometer) in a Hitachi S-4800 field emission scanning electron microscope (FESEM). Bulk densities of Ag (10.49 g/cm^3) and Au (19.3 g/cm^3) were used to calculate the film thicknesses from the k ratios measured for Ag Lα-lines and Au Mα-lines using a program GMRfilm.[87] FESEM was used to study microstructure of the deposited thin films. Crystal structures of the films were analyzed with a PANalytical X´Pert PRO MPD X-ray diffractometer. The measurements were performed in parallel beam geometry with copper Kα radiation (λ = 1.5406 Å). The incident angle was 1°. Four point probe measurements (Keithley 2400 SourceMeter with a Cascade Microtech four-point probe) were done for electrical characterization. Chemical composition of the films was analyzed with time-of-flight elastic recoil detection analysis (ToF-ERDA).[88]

Cross-sections of the Ag samples were prepared by Focused Ion Beam milling using a FEI Quanta 3D 200i DualBeam instrument. Images were taken with the Hitachi S-4800 FESEM. Thicknesses of the films were evaluated from the cross-section images.

4 Results and discussion

This chapter is based on references I-VII. Subchapters 4.1 and 4.2 summarize the results of the developed processes of Ag and Au thin films. In all the studies several metal compounds were first preliminarily evaluated for ALD by studying their thermal properties. The most promising compounds, one in each study, were chosen for the ALD experiments. Thickness, crystal structure, microstructure and composition were analyzed from the deposited thin films. There are also some non-published results considering mostly Au(N(SiMe3)2)(PEt3) applied with O3.

In Chapter 4.3 results from the two potential applications of Ag deposited by PEALD are discussed. The most important findings of these studies are presented.

4.1 Silver

Precursor characterization.

Six silver compounds being (2,2,6,6-tetramethylheptane-3,5-dionato)-(triethylphosphine)silver(I) (Ag(thd)(PEt_3)), (6,6,7,7,8,8,8-heptafluoro-2,2-dimethyl-3,5-octanedionato)silver(I) (Ag(fod)), (2,2-dimethylpropionato)silver(I) (Ag(piv)), (2,2-dimethylpropionato)(triethylphopshine)silver(I) (Ag(piv)(PEt_3)), (hexa-fluoroacetylacetonate)(trimethylphosphine)silver(I) (Ag(hfac)(PMe_3)), and Ag(fod)(PEt_3) (Figure 12) were evaluated for ALD. TGA curve proved Ag(fod)(PEt_3) as the most potential for ALD (Figure 13). TGA curve of Ag(fod)(PEt_3) showed a single step evaporation with 6 % residue while the Ag content of the compound is 22.7 %. Weight loss started at 110 °C and was complete at approximately 270 °C. The other compounds, including also Ag(hfac)(PMe_3) which has been used in thermal ALD of Ag thin films at

200 °C[82], left residues that were larger or equal to the content of Ag in the compound, thereby showing thermal decomposition.[I]

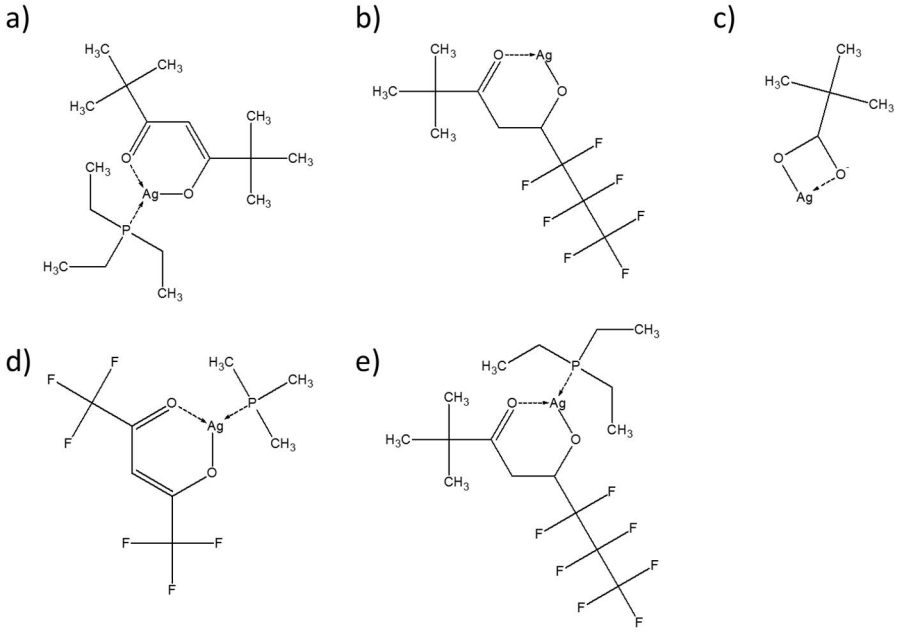

Figure 12. Molecular structures of the Ag compounds considered for PEALD of Ag thin films. a) Ag(thd)(PEt_3), b) Ag(fod), c) Ag(piv), d) Ag(hfac)(PMe_3) e) Ag(fod)(PEt_3).

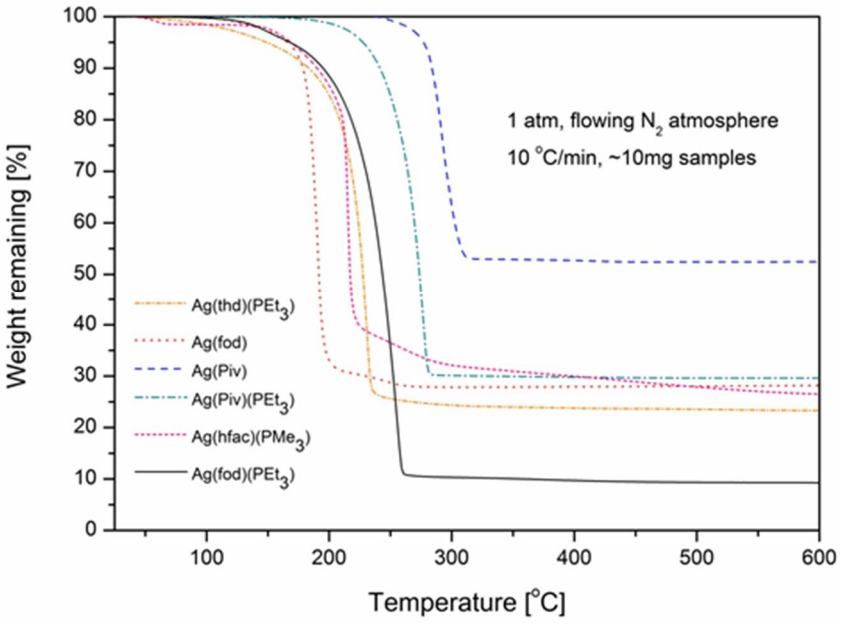

Figure 13. TGA curves of the studied Ag compounds. Reprinted from Chemistry of Materials, vol. 23, pages 2901-2907, M. Kariniemi et al.: "*Plasma-enhanced atomic layer deposition of Ag thin films",* Copyright (2011), American Chemical Society. http://pubs.acs.org/doi/10.1021/cm200402j

Film deposition.

In the PEALD process plasma activated hydrogen was used as a reducing agent. It was concluded that the growth of Ag was well enough self-limiting at 120 – 140 °C to be called as ALD (Figure 14a). At 120 °C the growth rate was 0.3 Å/cycle. At 140 °C there were already slight signs of thermal decomposition of Ag(fod)(PEt_3): uniformity of the films decreased, and the growth rate increased especially with the longer Ag(fod)(PEt_3) pulses. The effect of the plasma pulse length to the growth rate of Ag was also studied. The growth rate was slightly lower (0.27 Å/cycle) with 3 s pulses compared to the growth rate of 0.33 Å/cycle with 5 s plasma pulses.[I]

In the thermal ALD process of Ag thin films, $BH_3(NHMe_2)$ was applied as a reducing agent. The effect of the Ag(fod)(PEt_3) pulse length to the growth rate was studied at 110 °C proving the growth self-limiting in respect to the silver precursor pulse length (Figure 14b). The growth rate was 0.30 Å/cycle. At 130 °C the growth rate of Ag was already higher, 0.35 Å/cycle, maybe showing thermal decomposition but the effect of the Ag(fod)(PEt_3) pulse length to the growth rate of Ag was not studied at 130 °C or higher temperatures. The ALD temperature ranges determined for PEALD and thermal ALD are quite similar as expected and differences can be explained by the reactor design differences. Surface density of chemisorbed Ag(fod)(PEt_3) was most likely limiting the growth rate of Ag.[III]

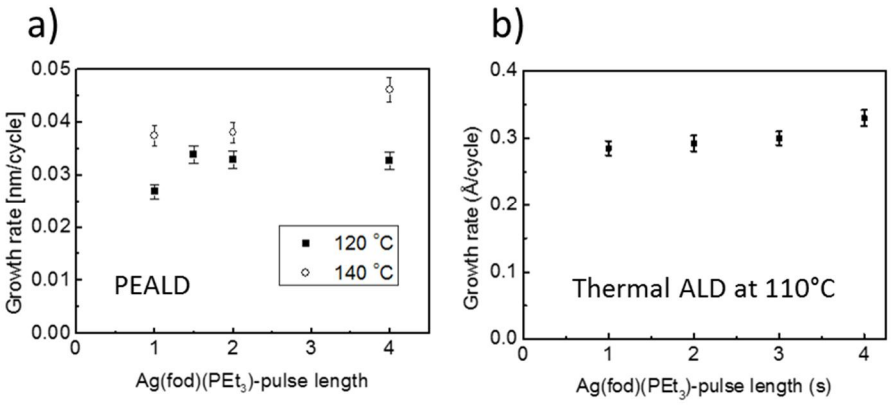

Figure 14. Growth rate of Ag as a function of Ag(fod)(PEt_3) pulse length in the studied processes. a) At temperatures 120 and 140 °C in the PEALD process. 500 cycles were applied with a 5 plasma pulses. b) At 110 °C in the thermal ALD process. 1000 cycles were applied with 1 s $BH_3(NHMe_2)$ pulses. Images modified and reprinted from Chemistry of Materials, vol. 23, pages 2901-2907, M. Kariniemi et al.: "*Plasma-enhanced atomic layer deposition of Ag thin films",* Copyright (2011), American Chemical Society, http://pubs.acs.org/doi/10.1021/cm200402j; and from Chemistry of Materials, vol. 29, pages 2040-2045, M. Mäkelä et al.: "*Studies on thermal atomic layer deposition of silver thin films",* Copyright (2017), American Chemical Society, http://pubs.acs.org/doi/abs/10.1021/acs.chemmater.6b04029

The results showed that Ag(fod)(PEt_3) started to decompose already around 130 – 140 °C even though TGA showed that it could be thermally stable up to 240 °C. It was proposed that the stability of Ag(fod)(PEt_3) as a liquid is different compared to the stability in gas phase and adsorbed on a surface.[I]

The ALD temperature ranges of the developed Ag processes are narrow, because the evaporation temperature of Ag(fod)(PEt_3) was 106 °C in the reactor used for the PEALD process and 95 °C in the thermal ALD reactor. Still, the processes were well controllable and Ag(fod)(PEt_3) was found at least as good Ag precursor for ALD as the other Ag precursors studied so far (Chapter 2.4.2).[6,79-82]

In the thermal ALD process of Ag(fod)(PEt_3) and $BH_3(NHMe_2)$ it was noticed that the amount of Ag deposited on the substrate surface affected the growth. At first, with 100 and 300 cycles, the growth rate of Ag was 0.18 Å/cycle on a Si(100) substrate. With more cycles, the growth rate started to increase until it stabilized to around 0.36 Å/cycle with 1500 or more cycles (Figure 15). In

addition, it was noticed that when a Ag thin film was deposited on a previously deposited Ag thin film the growth rate was clearly higher compared to a case where the same number of cycles were applied on a bare Si(100) substrate. The growth rate of Ag on a 73 nm thick Ag coating was 0.34 Å/cycle whereas on the bare Si(100) the growth rate was 0.29 Å/cycle (1000 cycles). On the previously deposited Ag the growth rate was thus very similar to the growth rate of Ag on Si when 1500 or more cycles were applied (0.36 Å/cycle) (Figure 15).[III]

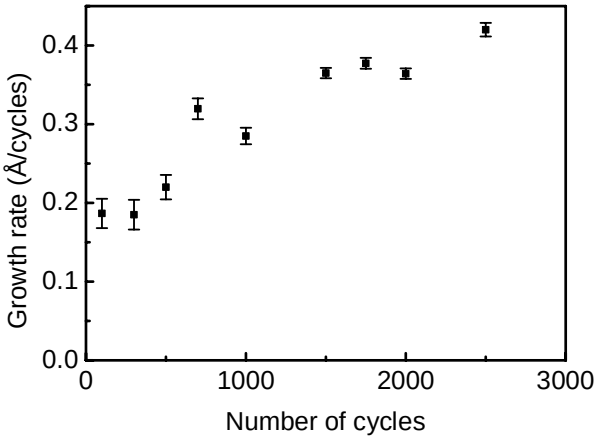

Figure 15. The effect of the cycle number on the growth rate of Ag in the thermal process of Ag(fod)(PEt_3) and $BH_3(NHMe_2)$. Depositions were performed at 110 °C with 1 s precursor pulses and purges. Reprinted from Chemistry of Materials, vol. 29, pages 2040-2045, M. Mäkelä et al.: "*Studies on thermal atomic layer deposition of silver thin films",* Copyright (2017), American Chemical Society, http://pubs.acs.org/doi/abs/10.1021/acs.chemmater.6b04029

The effect of the Ag surface to the Ag growth was explained by the reduction mechanism of $BH_3(NHMe_2)$. It was proposed that $BH_3(NHMe_2)$ reacted catalytically on Ag to $[Me_2N\text{-}BH_2]_2$ and H_2. This kind of dehydrogenation of $BH_3(NHMe_2)$ is common in solutions when there is a metal catalyst present.[89] It is also known that $BH_3(NHMe_2)$ is unlikely to dehydrogenate in vacuum irrespective of temperature when there is no metal catalyst present. [87] This is the case in an ALD reactor without any catalytic material like Ag. Kalutarage et al.[76,77] who used $BH_3(NHMe_2)$ as a reducing agent in ALD deposition of transition metal thin films including Cu, Ni, Co, Fe, Mn and Cr, proposed that at least at temperatures of 150 and 180 °C $BH_3(NHMe_2)$ adsorbs on a catalytic Ru and decomposes to reactive surface groups which are strong

reducing agents. In that study there was no growth of transition metals on bare Si substrates. Growth was observed only on Ru substrates. Like Ru, Ag is known for its catalytic properties.[90]

When depositing Ag thin films from Ag(fod)(PEt_3) and $BH_3(NHMe_2)$ it was noticed that not only reductive surface species were formed on catalytic surfaces from $BH_3(NHMe_2)$ but also desorbing species were formed. When catalytic Ru substrates were placed in the reaction chamber in front of the bare Si substrate the growth rate of Ag was clearly higher on Si compared to a study where there was no Ru in the chamber. This led to a conclusion that also species which desorbed from Ru were created from $BH_3(NHMe_2)$. To study this observation in more detail, Ru pieces were placed into the source tube of $BH_3(NHMe_2)$. This is possible in the ASM F120 ALD reactor where $BH_3(NHMe_2)$ was held in a glass boat inside its own source tube. By inserting Ru to the source tube of $BH_3(NHMe_2)$ the effect of Ru to Ag(fod)(PEt_3) was excluded. In these experiments the growth rate of Ag was clearly higher on Si compared to a case where no Ru catalyst was present in the reactor (Figure 16). At 110 °C the growth rate of Ag on Si was 0.29 Å/cycle when 1000 cycles were applied without Ru whereas it was 0.33 Å/cycle when Ru pieces were in the source tube of $BH_3(NHMe_2)$. At deposition temperature of 130 °C differences in the growth rates are non-distinguishable, most likely because of the onset of the thermal decomposition of Ag(fod)(PEt_3). These tests proved that on Ru more reductive or reactive species were formed from $BH_3(NHMe_2)$.[III]

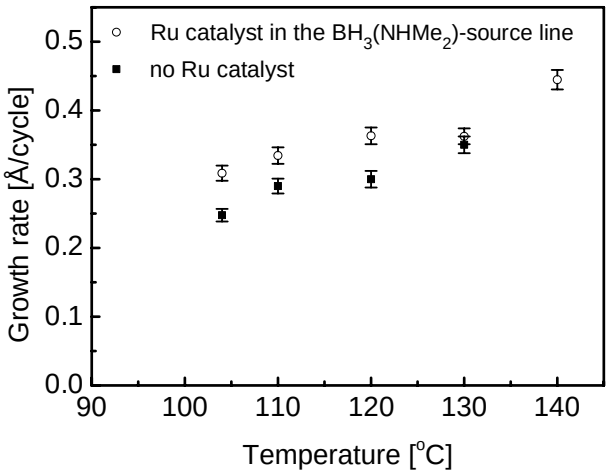

Figure 16. The growth rate of Ag as a function of the deposition temperature without a Ru catalyst (closed circles) and with a Ru catalyst in the source tube of $BH_3(NHMe_2)$ (open circles). 1000 cycles were applied with 1 s precursor pulses and purges. Reprinted from Chemistry of Materials, vol. 29, pages 2040-2045, M. Mäkelä et al.: "*Studies on thermal atomic layer deposition of silver thin films",* Copyright (2017), American Chemical Society.
http://pubs.acs.org/doi/abs/10.1021/acs.chemmater.6b04029

It was also studied wether the possibly forming H_2 can reduce chemisorbed $Ag(fod)(PEt_3)$. At 110 °C 1500 cycles of 1 s $Ag(fod)(PEt_3)$ pulses and 4 s H_2 pulses were applied. This resulted in a Ag thin film with a nominal thickness of only 1 nm as analyzed by EDS. This showed that H_2 is not reactive enough for the reduction of chemisorbed $Ag(fod)(PEt_3)$.

It remained as an open question, how the growth started on Si(100) when $Ag(fod)(PEt_3)$ and $BH_3(NHMe_2)$ were applied. It can be proposed that $BH_3(NHMe_2)$ reduced chemisorbed $Ag(fod)(PEt_3)$ at first but then, after formation of small nanoparticles of Ag on Si, the activation of $BH_3(NHMe_2)$ to more reactive species started and reductive species changed. It can also be proposed that $Ag(fod)(PEt_3)$ decomposed slightly to Ag and launched the activation of $BH_3(NHMe_2)$. If this is true, the actual reduction power of $BH_3(NHMe_2)$ itself stays unclear. It has been speculated that minor decomposition of metal precursors is required also for the nucleation of noble metal thin films when these are deposited with oxygen as a co-reactant in ALD.[2]

It was unclear what happened to $BH_3(NHMe_2)$ when its pulse length was varied because the growth rate did not stay constant as a function of the $BH_3(NHMe_2)$ pulse length at 110 °C (Figure 17). Instead it increased from 0.29 Å/cycle to a level of 0.40 Å/cycle with 2 and 3 s pulses, but again dropped to 0.34 Å/cycle with 4 s pulse. The maximum non-uniformity of these films was 10 % when the film thickness was 38 nm. If one wants to propose something, it can be proposed that when $BH_3(NHMe_2)$ accompanied with its derivatives was pulsed to the chamber, it first reacted with the ligands of the chemisorbed $Ag(fod)(PEt_3)$ and produced metallic Ag surface. If the exposure time was long enough (over 2 s), the metallic Ag surface was saturated with stable and reactive surface groups formed by $BH_3(NHMe_2)$. After the purge, these surface groups reacted with the next pulse of $Ag(fod)(PEt_3)$ and reduced it to Ag. $Ag(fod)(PEt_3)$ also chemisorbed to Ag surface if the exposure time was long enough. Again, after the purge period, $BH_3(NHMe_2)$ reacted with the ligands of the chemisorbed $Ag(fod)(PEt_3)$. When the exposure time of $BH_3(NHMe_2)$ was less than 2 s, $BH_3(NHMe_2)$ did not have enough time to saturate the surface with the stable surface groups. It only had time to react with the ligands of the chemisorbed $Ag(fod)(PEt_3)$ leading to a lower growth rate compared to a case when the stable surface groups were created. Similar arguments were proposed when the growth rates of Ag deposited from $Ag(fod)(PEt_3)$ and plasma-activated H_2 or NH_3 were compared. Application of plasma-activated NH_3 resulted in clearly higher growth rates of Ag than application of plasma-activated H_2.[9,91] The presented theory does not explain why the growth rate decreased when even longer 4 s $BH_3(NHMe_2)$ pulses were used. To be sure about the results, these depositions should be done again. It should still be mentioned that in the ALD papers considering $BH_3(NHMe_2)$ as a reducing agent the self-limiting growth has been shown on catalytic surfaces at 150 and 180 °C in respect to $BH_3(NHMe_2)$ pulse length when non-catalytic metals were deposited.[76,77]

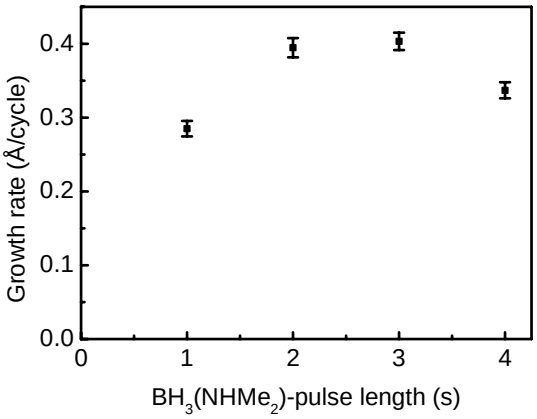

Figure 17. The growth rate of Ag as a function of $BH_3(NHMe_2)$ pulse length at 110 °C. The $Ag(fod)(PEt_3)$ pulse length was 1 s. Reprinted from Chemistry of Materials, vol. 29, pages 2040-2045, M. Mäkelä et al.: "*Studies on thermal atomic layer deposition of silver thin films",* Copyright (2017), American Chemical Society. http://pubs.acs.org/doi/abs/10.1021/acs.chemmater.6b04029

As a conclusion, in the studied thermal ALD Ag process the growth was self-limiting in respect to the $Ag(fod)(PEt_3)$ pulse but not quite to the $BH_3(NHMe_2)$ pulse. To be called true ALD the process should show self-limiting growth in respect to both precursors.

Film properties.

The developed two Ag processes produced Ag thin films with different properties. The PEALD process resulted in mirror like thin films on Si and glass whereas the thermal process produced coatings which had matte appearance on Si and glass.

It was concluded that in the PEALD process the film growth started by formation of nanoclusters which then grew in size and finally coalesced to a continuous thin film (Figure 18a). Films thinner than 10 nm were non-continuous.[I] The same nucleation behavior was noticed by Minjauw et al.[9] when Ag thin films were deposited from $Ag(fod)(PEt_3)$ and plasma activated H_2.

The thermally deposited Ag thin films were found to consist of particles and were non-continuous even after 2500 cycles were applied and the nominal film thickness was close to 100 nm. In the thicker films, there were smaller particles between the large particles which was a result of coalescence and continued nucleation (Figure 18b).[III] It is possible that when $BH_3(NHMe_2)$ is used as a reducing agent, the true reduction reaction is catalytic and more probable on Ag surface. However, also volatile reducing species are formed as proved by placing Ru pieces to the source tube of $BH_3(NHMe_2)$. These species could be expected to reduce chemisorbed $Ag(fod)(PEt_3)$ also on Si.

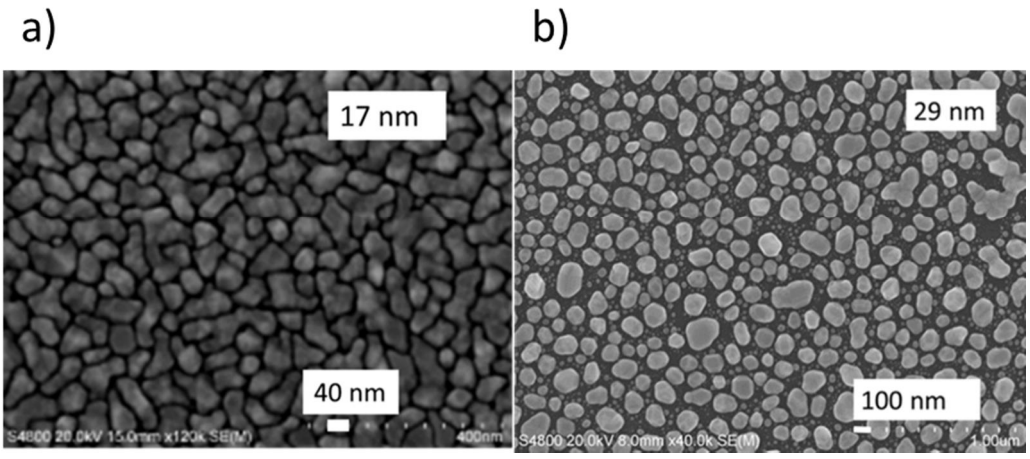

Figure 18. Microstructure of the Ag thin films deposited from $Ag(fod)(PEt_3)$ a) using the PEALD process with plasma activated H_2 b) using the thermal process with $BH_3(NHMe_2)$ as a reducing agent. The nominal film thicknesses are marked to the images. Images modified and reprinted from Chemistry of Materials, vol. 23, pages 2901-2907, M. Kariniemi et al.: "*Plasma-enhanced atomic layer deposition of Ag thin films",* Copyright (2011), American Chemical Society, http://pubs.acs.org/doi/10.1021/cm200402j; and from Chemistry of Materials, vol. 29, pages 2040-2045, M. Mäkelä et al.: "*Studies on thermal atomic layer deposition of silver thin films",* Copyright (2017), American Chemical Society. http://pubs.acs.org/doi/abs/10.1021/acs.chemmater.6b04029

All the Ag thin films deposited by both thermal and plasma-enhanced ALD were polycrystalline and exhibited a cubic Ag structure (Figure 19). Chemical composition of the Ag thin films deposited at 120 °C by PEALD and at 110 °C by thermal ALD were analyzed by ToF-ERDA. A 17 nm thick Ag thin film deposited by PEALD from $Ag(fod)(PEt_3)$ and plasma activated H_2 contained 85 at.% Ag, 7 at.% H, 3 at.% C, 3 at.% O, 0.9 at.% P, O.5 at.% F and 0.7 at.% N.[I] A 55 nm thick Ag thin film deposited by thermal ALD from $Ag(fod)(PEt_3)$

and $BH_3(NHMe_2)$ contained 97 at.% Ag, 1.6 at.% O, H 0.8 at.%, C 0.7 at.%.[III] The latter sample was stored in a desiccator before the measurement whereas the sample deposited by PEALD was stored in air. This can explain the differences in composition to some extent. The measurements were also performed with different ToF-ERD telescopes and ions. The PEALD sample was measured with 7.5 MeV $^{37}Cl^{4+}$ and the thermal ALD sample with 35 MeV $^{79}Br^{6+}$ ions. In both cases the surface roughness of the film was high compared to its thickness which spread the elemental distributions in the ToF-ERDA depth profiles.[I] The impurity contents analyzed for the PEALD Ag thin film are the upper limits.[I] Compared to the values reported for the other Ag ALD processes, the impurity levels of the films deposited by the two new Ag processes are very moderate.[6-9,80-82]

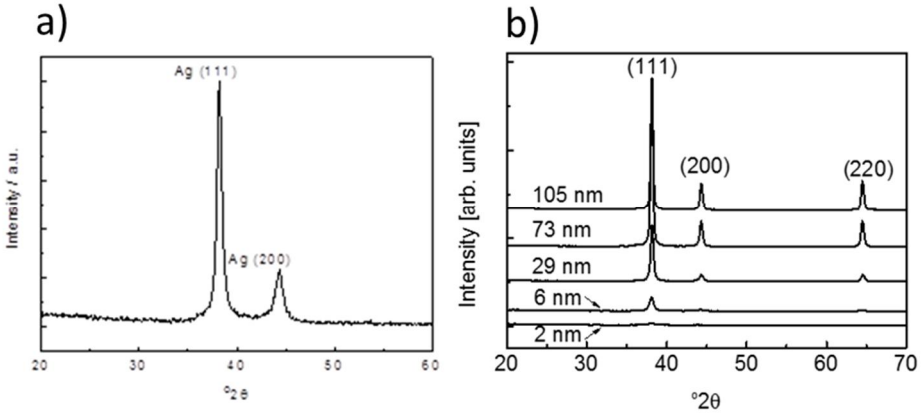

Figure 19. X-ray diffraction patterns of the Ag thin films deposited by a) PEALD process and b) thermal process. Thickness of the PEALD Ag thin film was 17 nm. In figure b) the thin film thicknesses are shown. All the thin films were deposited on Si(100) substrates. Images modified and reprinted from Chemistry of Materials, vol. 23, pages 2901-2907, M. Kariniemi et al.: "*Plasma-enhanced atomic layer deposition of Ag thin films",* Copyright (2011), American Chemical Society, http://pubs.acs.org/doi/10.1021/cm200402j; and from Chemistry of Materials, vol. 29, pages 2040-2045, M. Mäkelä et al.: "*Studies on thermal atomic layer deposition of silver thin films",* Copyright (2017), American Chemical Society, http://pubs.acs.org/doi/abs/10.1021/acs.chemmater.6b04029

Continuous Ag thin films deposited by PEALD were conductive. A 22 nm thick film exhibited resistivities of 6 – 8 μΩ·cm. This is a low resistivity for a chemically deposited thin film and can be compared to the resistivity of Ag achieved in a REALD study where a 40 nm thick film had a resistivity of 6

μΩ·cm.[6] Ag(fod)(PEt_3) has also been used in chemical vapor deposition (CVD) where the resistivities of the deposited Ag thin films have been 1.9 – 3 μΩ·cm.[92,93] Yuan et al.[92] reported resistivities of 2.5 – 3.0 μΩ·cm for 2 μm thick Ag films deposited at 230 and 320 °C using moist H_2 carrier gas. Gao et al.[93] reported resistivities of 1.9 – 3 μΩ·cm for Ag films deposited at 220 and 350 °C using H_2 carrier gas. In comparison to these other results the resistivity values achieved with the developed PEALD Ag process are good. When comparing the resistivity values reported for thin films, the effect of the film thickness should be considered. When the polycrystalline thin film is very thin the resistivity is always higher than in thicker film or in bulk because of increased interface and grain boundary scattering.[94,95]

Conformality of the Ag thin films deposited by PEALD was studied. As discussed in Chapter 2.2, in PEALD processes conformality is often limited because of the radical recombination on the walls of 3D structures. Factors affecting the probability of radical recombination include the substrate material and the reactive gas. The recombination loss probability is higher on metals than on oxides, and hydrogen radicals recombine more likely than oxygen or nitrogen radicals.[41] In the experiment Ag was deposited on deep trenches whose length was 6.75 μm and the opening 115 nm giving an aspect ratio of about 60:1. The trenches had either SiO_2 or TiN coating on the surface. All the deposition parameters were the same. No perfect conformality was achieved (Figure 20). First, deposition of a metal using plasma-activated H_2 as a reducing agent is difficult because of the high probability of hydrogen radicals to recombine especially on a growing metal surface. Secondly, the material on the trench affected the conformality. The film deposited on trenches with a SiO_2 surface had better conformality than the film deposited on trenches with a TiN surface. It is indeed expected that the radicals recombine faster on conductive TiN than on insulating SiO_2.[II]

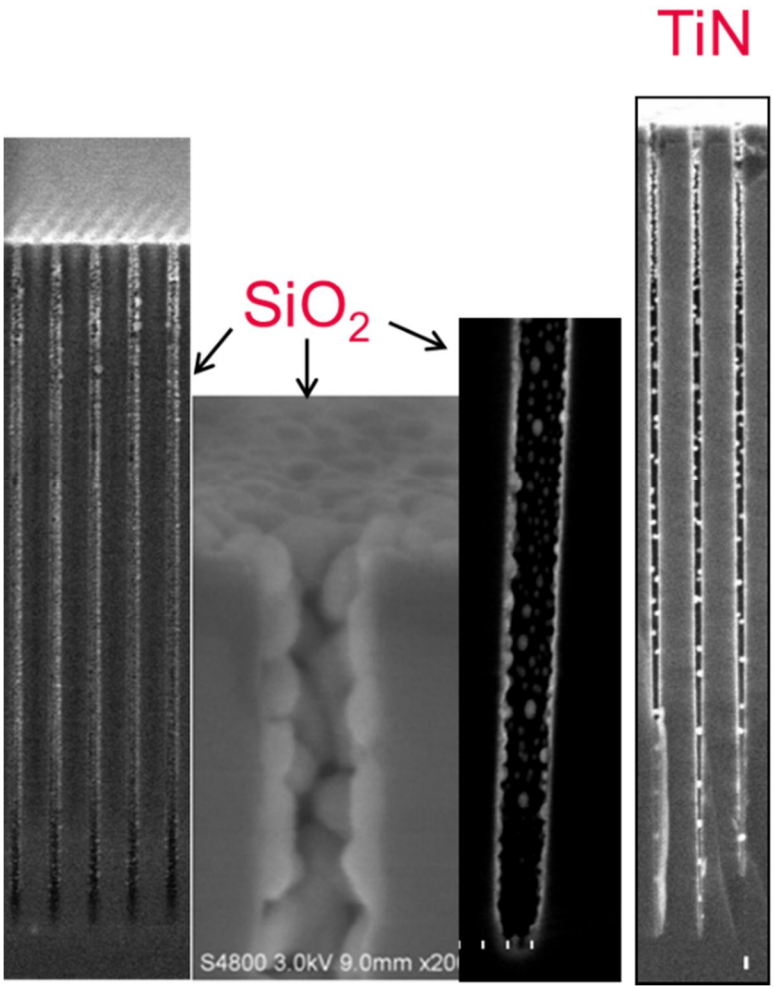

Figure 20. Ag thin films deposited onto porous trench structures by applying Ag(fod)(PEt_3) and plasma activated H_2. The length of a trench was 6.75 µm and the opening was 115 nm. Images are showing trenches with either a SiO_2 or TiN coating in the trench. Ag(fod)(PEt_3) pulse length was 5 s and the hydrogen plasma exposure time was 7 s. Reprinted from Journal of Vacuum Science and Technology A, vol. 30, page 01A115, M. Kariniemi et al.: "*Conformality of remote plasma-enhanced atomic layer deposition processes: An experimental study",* Copyright (2012), reproduced with permission from AIP Publishing LLC (American Vacuum Society). http://avs.scitation.org/doi/abs/10.1116/1.3659699?journalCode=jva

All the Ag thin films deposited on Si could be destroyed by scratching with tweezers or gloves. Scotch tape tests were performed and only the PEALD thin films thinner than 30 nm passed the test.[I] All the thermally deposited Ag thin films failed the tests.[III] For better adhesion a proper adhesion layer should be used. It was also noticed that all the deposited Ag thin films turned yellow over time in air. In the case of the thermally deposited Ag thin films also delamination was noticed unless the films were stored in a desiccator.

4.2 Gold

Precursor characterization.

Both Au(I) and Au(III) compounds were considered for ALD. In total seven Au(I) compounds were synthesized and preliminary evaluated for thermal ALD. These compounds were chloro(dimethylsulfide)gold ($AuCl(SMe_2)$), chloro(tetrahydrothiophene)gold ($AuCl(SC_4H_8)$), methyl(triethylphosphine)-gold ($MeAu(PEt_3)$), (diethyl-dithiocarbamate)(triethylphosphine)gold ($Au(S_2CNEt_2)(PEt_3)$), (2,2-dimethyl-6,6,7,7,8,8,8-heptafluorooctane-3,5-dionato)(triethylphosphine)gold ($Au(fod)(PEt_3)$), (bis(trimethylsilyl)-amido(triethylphosphine)gold ($Au(N(SiMe_3)_2)(PEt_3)$) and chloro(tri-ethylphosphine)gold ($AuCl(PEt_3)$) (Figure 21).[V]

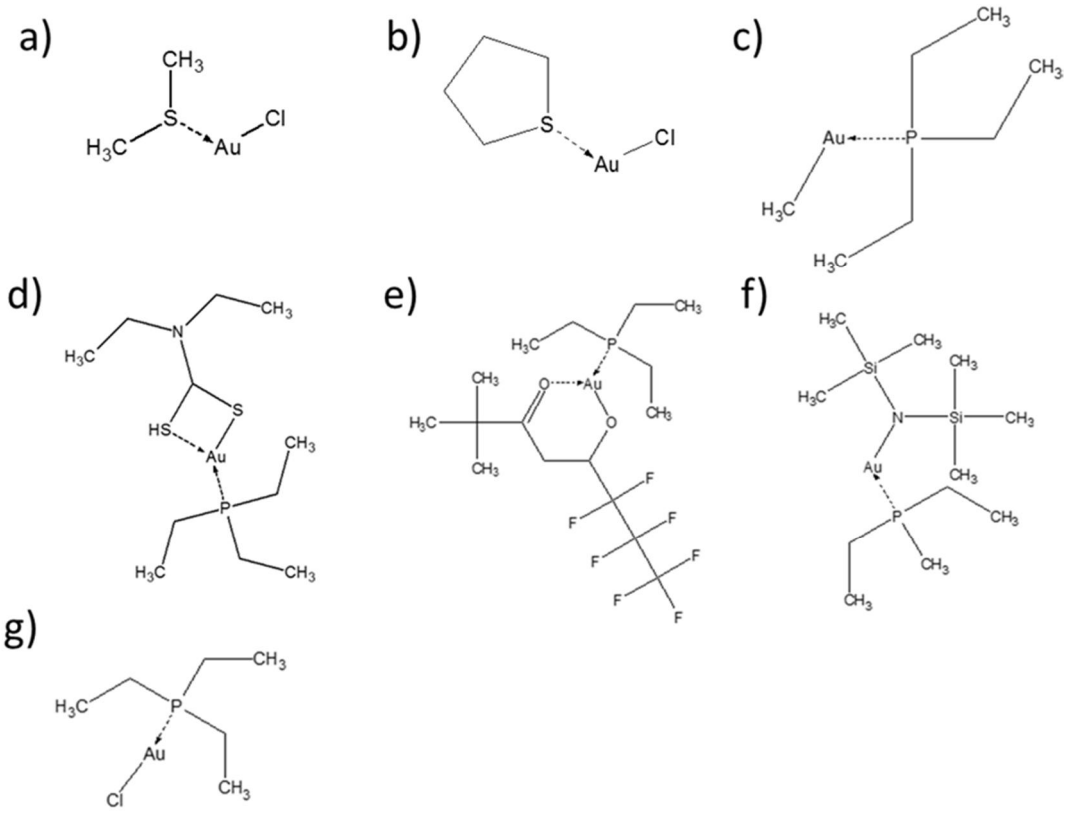

Figure 21. Schematic pictures of the Au(I) compounds studied. a) $AuCl(SMe_2)$, b) $AuCl(SC_4H_8)$, c) $MeAu(PEt_3)$, d) $Au(S_2CNEt_2)(PEt_3)$, e) $Au(fod)(PEt_3)$, f) $Au(N(SiMe_3)_2)(PEt_3)$ and g) $AuCl(PEt_3)$.

TGA showed that most of the Au(I) compounds decomposed when heated (Figure 22). Only three of the compounds showed some potential for ALD. $Au(N(SiMe_3)_2)(PEt_3)$ left a residue of 26.5 % while the theoretical Au content was 41.4 %. $Au(fod)(PEt_3)$ left a residue of 23.8 % while the theoretical Au content was 32.2 %. $AuCl(PEt_3)$ left a residue of 30.6 % while the theoretical Au content was 56.2 %. None of the precursors was truly promising for ALD where a single step evaporation with zero residual mass is desired. However, $Au(N(SiMe_3)_2)(PEt_3)$ was chosen for the deposition experiments because of the low evaporation temperature (61 °C) combined with reasonably good thermal properties.[V]

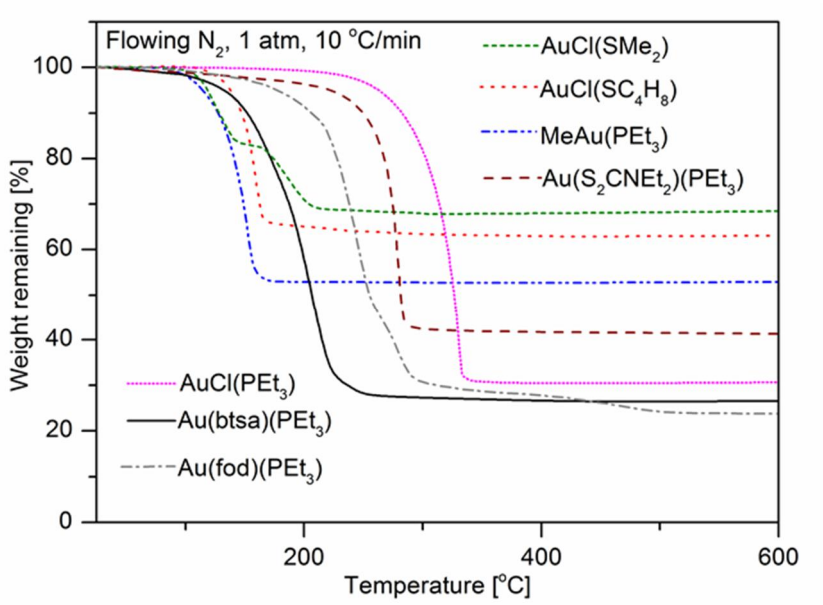

Figure 22. TGA curves of the studied Au(I) compounds. Reprinted from Journal of Vacuum Science and Technology A, vol. 35, page 01B112, M. Mäkelä et al.: *"Potential gold(I) precursors evaluated for atomic layer deposition"*, Copyright (2012), reproduced with permission from AIP Publishing LLC (American Vacuum Society).
http://avs.scitation.org/doi/abs/10.1116/1.4968193?journalCode=jva

Five Au(III) compounds were evaluated for ALD. The studied compounds were gold chloride ($AuCl_3$), (dichloro)(diethylthiocarbamato)gold ($AuCl_2(S_2CNEt_2)$), dimethylacetatogold ($Me_2Au(OAc)$), dimethyl(4-(methylimino)pent-2-en-2-olato)gold ($Me_2Au(Nacac)$ and dimethyl(diethylthiocarbamato)gold ($Me_2Au(S_2CNEt_2)$) (Figure 23).[IV]

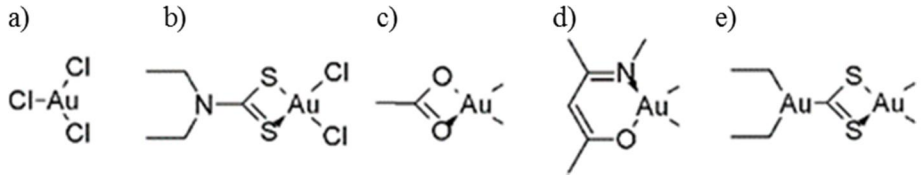

Figure 23. Schematic pictures of the Au(III) compounds studied. a) $AuCl_3$, b) $AuCl_2(S_2CNEt_2)$ c) $Me_2Au(OAc)$, d) $Me_2Au(Nacac)$ and e) $Me_2Au(S_2CNEt_2)$. Reprinted from Chemistry of Materials, vol. 29, pages 6130-6136, M. Mäkelä et al.: "*Thermal atomic layer deposition of continuous and highly conducting gold thin films",* Copyright (2017), reproduced with permission from American Chemical Society. http://pubs.acs.org/doi/abs/10.1021/acs.chemmater.7b02167

TGA of the compounds showed that $Me_2Au(S_2CNEt_2)$ was clearly different from all the other Au(III) compunds studied. It was also different from all the Au(I) compounds studied. As wanted in ALD, $Me_2Au(S_2CNEt_2)$ evaporated in a single step leaving almost zero residual mass (Figure 24).[IV]

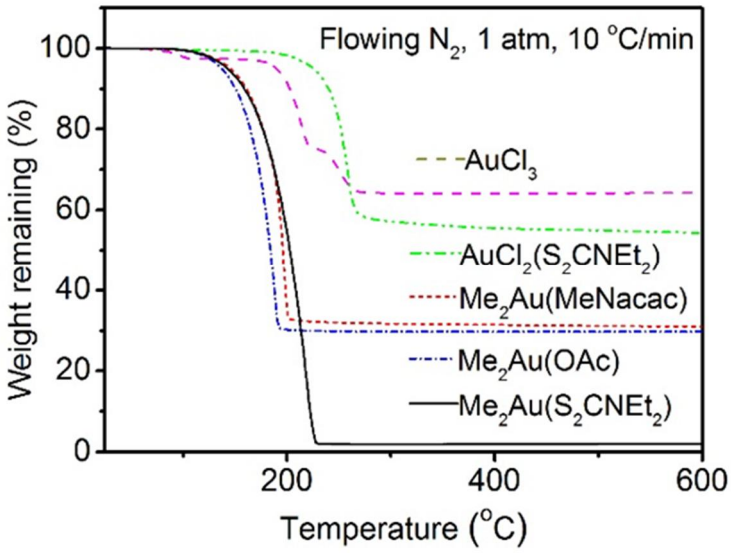

Figure 24. TGA curves of the studied Au(III) compounds. Reprinted from Chemistry of Materials, vol. 29, pages 6130-6136, M. Mäkelä et al.: "*Thermal atomic layer deposition of continuous and highly conducting gold thin films",* Copyright (2017), reproduced with permission from American Chemical Society. http://pubs.acs.org/doi/abs/10.1021/acs.chemmater.7b02167

Film deposition and properties.

Both Au compounds selected for the growth experiments were combined with O_3. Noble metal thin films are often deposited by application of O_2 or O_3 as a co-reactant as introduced in Chapter 2.4.1. These processes are combustion type and produce noble metal thin films typically at temperatures above 200 °C where the corresponding noble metal oxides are not stable.[14,19] Au_2O_3 is expected to decompose around 170 °C with a possible Au_2O intermediate.[IV,66] Similar approach was also tried by combining $Au(N(SiMe_3)_2)(PEt_3)$ with H_2S. This could result in formation of Au sulfides (Au_2S and Au_2S_3). Decomposition temperature of Au_2S_3 precipitate is around 200 °C[V,96] and of Au_2S precipitate 147 – 220 °C.[V,97] The benefit of applying O_3 or H_2S with the Au precursor is that these are common co-reactants in ALD processes and easily-implemented to any reactor. However, it should be noticed that H_2S is harmful and in excessive amounts very toxic.

4.2.1 $Me_2Au(S_2CNEt_2)$ as a precursor

$Me_2Au(S_2CNEt_2)$ was tested with O_3 at 120 – 250 °C to study its thermal stability. At 250 °C it clearly decomposed already in the source tube before reaching the reaction chamber but at lower temperatures there were no signs of thermal decomposition. Instead the Au thin films deposited were shiny and very uniform in thickness over the 5 x 5 cm^2 area. However, at 120 and 150 °C there were some circular marks in the thin films (Figure 25). These were interpreted as a sign of ineffective decomposition of gold oxide.

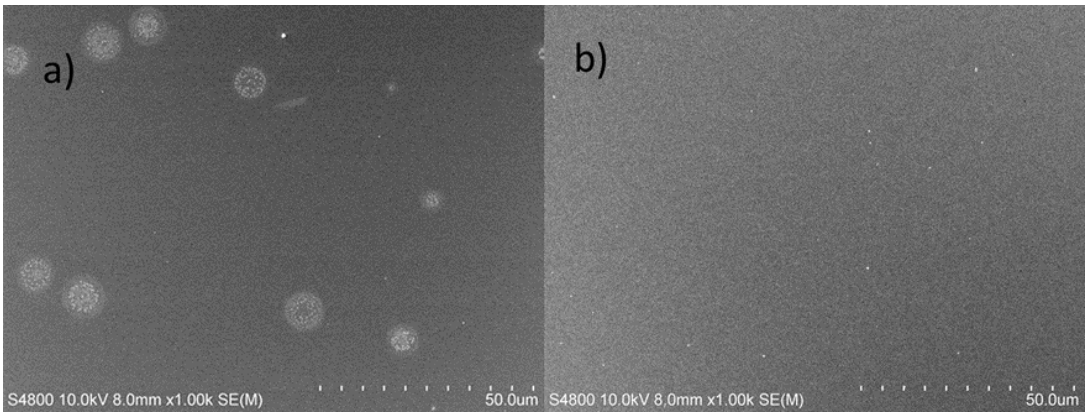

Figure 25. FESEM images of the Au thin films deposited from $Me_2Au(S_2CNEt_2)$ and O_3 at a) 120 °C and b) 200 °C with the same deposition parameters. The film deposited at 120 °C was 21 nm thick and the film deposited at 200 °C was 56 nm thick.

The growth rate of Au increased from 0.4 to 1.1 Å/cycle as a function of deposition temperature from 120 to 200 °C (Figure 26a). Often the increase of the growth rate with temperature is a sign of precursor decomposition but in the case of noble metals and noble metal oxides this is common and still the growth can be self-limiting as characteristic to ALD. Active oxygen staying on noble metal surfaces can affect the growth rate at different temperatures (Chapter 2.1).[14,16-18,65] The self-limiting growth of Au was confirmed at 180 °C by varying the $Me_2Au(S_2CNEt_2)$ pulse length from 0.5 to 2 s. The growth rate was 0.9 Å/cycle (Figure 26b).[IV]

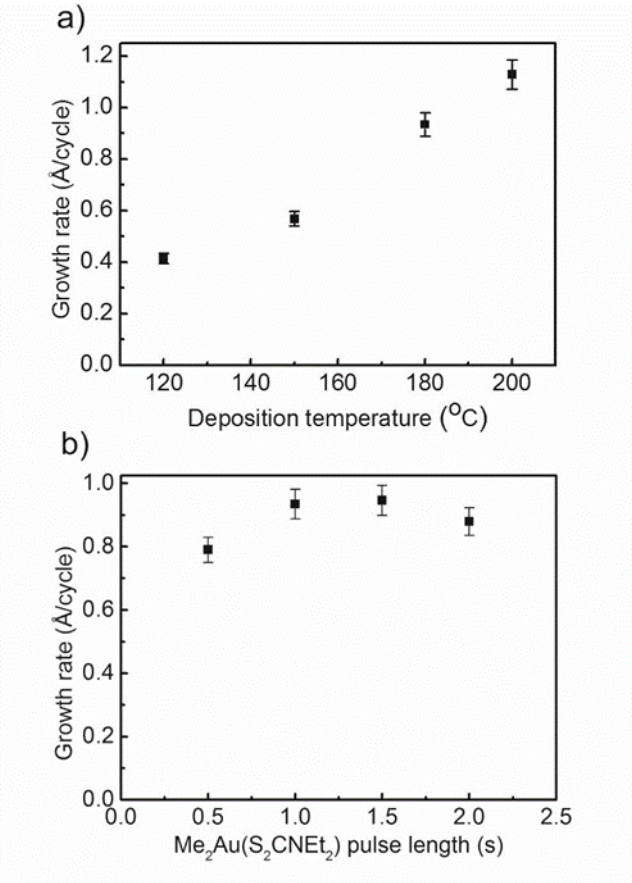

Figure 26. a) The growth rate of Au at deposition temperatures 120 – 200 °C. The $Me_2Au(S_2CNEt_2)$ and O_3 pulse lengths were 1 s. b) Growth rate of Au as a function of $Me_2Au(S_2CNEt_2)$ pulse length at 180 °C. Reprinted from Chemistry of Materials, vol. 29, pages 6130-6136, M. Mäkelä et al.: "*Thermal atomic layer deposition of continuous and highly conducting gold thin films",* Copyright (2017), reproduced with permission from American Chemical Society. http://pubs.acs.org/doi/abs/10.1021/acs.chemmater.7b02167

The achieved growth rate of Au thin films can be compared to the only one previously published ALD process of Au.[10] When $Me_3Au(PMe_3)$ and plasma activated O_2 and water were used the growth rate of Au was 0.5 Å/cycle at 130 °C. Around 130 °C the growth rates are thus similar in both processes. Above 130 °C $Me_3Au(PMe_3)$ decomposed. Thermal routes to Au thin films were also tried with $Me_3Au(PMe_3)$. There was no growth when either O_3, H_2O or molecular O_2 were applied at temperatures below 130 °C showing $Me_2Au(S_2CNEt_2)$ to be more reactive than $Me_3Au(PMe_3)$.

All the deposited Au thin films were polycrystalline and showed the cubic phase of gold (Figure 27a). FESEM studies showed that the films were continuous although there were some gaps between the grains (Figure 27b).

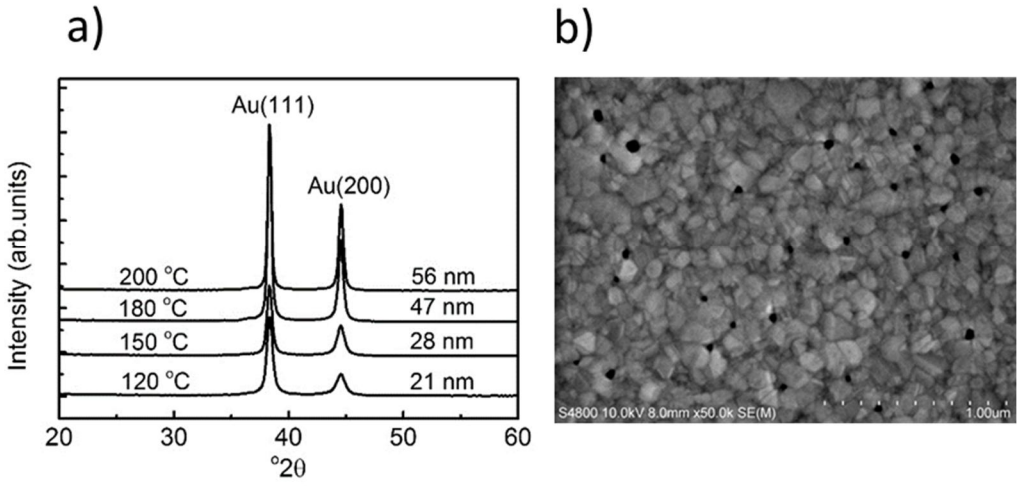

Figure 27. a) XRD patterns of the Au thin films deposited at 120 – 200 °C from $Me_2Au(S_2CNEt_2)$ and O_3 with 1 s pulse lengths. 500 cycles were applied. Film thicknesses are marked to the image. b) FESEM image of the Au thin film deposited with $Me_2Au(S_2CNEt_2)$ and O_3 at 180 °C. The nominal film thickness was 47 nm. Reprinted from Chemistry of Materials, vol. 29, pages 6130-6136, M. Mäkelä et al.: "*Thermal atomic layer deposition of continuous and highly conducting gold thin films",* Copyright (2017), reproduced with permission from American Chemical Society. http://pubs.acs.org/doi/abs/10.1021/acs.chemmater.7b02167

Compositions of the Au thin films were analyzed by TOF-ERDA. A film deposited at 120 °C was first analyzed. This 20 nm thick Au thin film consisted of Au (91.2 at.%), O (5.3 at.%), H (2.2 at.%), C (0.9 at.%) and N (0.5 at.%). Slightly lower impurity contents (O 2.9 at.%, H 0.9 at.%, C 0.2 at.% and N 0.2 at.%) were analyzed from a film which was 47 nm thick and was deposited at 180 °C. These two analyzed Au thin films were otherwise deposited with the same parameters and with the precursor pulses of 1 s. TOF-ERD analysis showed that most likely the circular marks noticed by eye in the films deposited at 120 and 150 °C were oxide impurities. No sulfur was found from the Au thin films even if the S_2CNEt_2 ligand is bonded to gold through sulfur donor atoms. The impurity levels of the analyzed Au thin films were typical for noble metal thin films deposited by ALD using O_2 or O_3 as a reactant.[IV,19]

The Au thin films were electrically conductive and showed low resistivity on glass. The resistivity values were in the range of 4.5 – 17 μΩ·cm for the Au films deposited at 180 °C and having thicknesses of 40 – 47 nm. The literature value for the Au resistivity is 2.44 μ·Ωcm. These films can also be compared to a 200 nm thick Au film deposited by CVD from trifluorophosphine gold(I) chloride and H_2 at 110 °C which had a resistivity of 9.6 μΩ·cm.[IV,98] An 80 nm Au film deposited by plasma-CVD had a resistivity of 4.6 μΩ·cm.[IV,99] These examples show that the resistivity values achieved with $Me_2Au(S_2CNEt_2)$ compare well with the resistivity values reported for other chemically deposited Au thin films.[IV]

4.2.2 $Au(N(SiMe_3)_2)(PEt_3)$ as a precursor

Application of $Au(N(SiMe_3)_2)(PEt_3)$ and O_3 at 120 ºC resulted in Au thin films with a growth rate of 0.02 Å/cycle which is too low for a reasonable ALD process. Neither application of H_2S with $Au(N(SiMe_3)_2)(PEt_3)$ at 150 – 160 ºC was successful. Only minimal Au particles were gained on Si(100) and glass when 1000 cycles of $Au(N(SiMe_3)_2)(PEt_3)$ and H_2S were pulsed.[V]

In addition to O_3 and H_2S, $Au(N(SiMe_3)_2)(PEt_3)$ was also tested with true reducing agents being triethylsilane (Et_3SiH), hydroquinone (benezene-1,4-diol), trimethylamine borane $BH_3(NMe_3)$ and $BH_3(NHMe_2)$. Et_3SiH was considered because of its Si-H group which could be reducing. It still safer to apply to ALD processes than pure silanes which are pyrophoric in air. Hydroquinone can oxidize to benzoquinone in redox reactions.[V] It has been used in determination of Au from solutions,[101] in nanoparticle synthesis in solutions and in electroless thin film growth.[V,101,102] Depositions with the reducing agents were performed at 150 – 160 °C. Application of $BH_3(NHMe_2)$ and hydroquinone resulted in shiny Au thin films on Si(100) and glass, but with $BH_3(NMe_3)$ and Et_3SiH there was almost no growth on these substrates. The growth rates of Au achieved with $BH_3(NHMe_2)$ and hydroquinone were quite similar and low (around 0.06 Å/cycle) at 150 °C but deposition were continued with $BH_3(NHMe_2)$.[V]

In the processes where $Au(N(SiMe_3)_2)(PEt_3)$ and $BH_3(NHMe_2)$ were alternately pulsed, the growth rate of Au was around 0.05 – 0.06 Å/cycle at temperatures of 80 – 140 °C. At 160 °C the growth rate increased considerably to 0.11 Å/cycle (Figure 28a).[V]

The effect of the $Au(N(SiMe_3)_2)(PEt_3)$ pulse length was studied at 100 °C. It was noticed that the growth rate increased as a function of the $Au(N(SiMe_3)_2)(PEt_3)$ pulse length (Figure 28b). However, it was confirmed that even at 150 °C there was no growth when $Au(N(SiMe_3)_2)(PEt_3)$ was pulsed alone without any reactant on Si, glass, Ru and Au substrates. This shows that the possible decomposition of $Au(N(SiMe_3)_2)(PEt_3)$ was very moderate. It can also be assumed that no constant growth rate was achieved due to slow surface reactions. The effect of the $BH_3(NHMe_2)$ pulse length to the growth rate of Au was studied at 100 °C. The growth rate was constant and around 0.07 Å/cycle.[V]

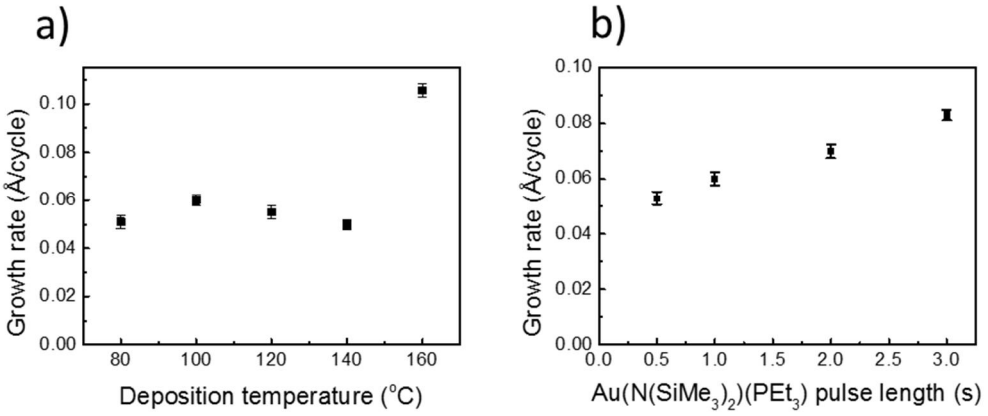

Figure 28. a) Growth rate of Au at 80 – 160 °C. b) Growth rate of Au as a function of the $Au(N(SiMe_3)_2)(PEt_3)$ pulse length at 100 °C. In all the depositions the $BH_3(NHMe_2)$ pulse length was 1 s. Reprinted from Journal of Vacuum Science and Technology A, vol. 35, page 01B112, M. Mäkelä et al.: *"Potential gold(I) precursors evaluated for atomic layer deposition"*, Copyright (2012), reproduced with permission from AIP Publishing LLC (American Vacuum Society). http://avs.scitation.org/doi/abs/10.1116/1.4968193?journalCode=jva

Major difficulty in the developed process with $Au(N(SiMe_3)_2)(PEt_3)$ and $BH_3(NHMe_2)$ was that the growth was very slow. It was also noticed that at 100 °C the growth rate of Au decreased as a function of applied cycles after a certain film thickness. The growth rate was 0.075 Å/cycle with 500 and 1000 cycles whereas 2408 cycles resulted in a growth rate of 0.06 Å/cycle. This phenomenon was also noticed at 120 °C when Au was deposited on itself as compared to starting with a bare Si substrate. On Si the growth rate was 0.055 Å/cycle but on Au particles only 0.03 Å/cycle. But then, at 160 °C the growth rate increased with increasing number of deposition cycles after a certain Au film thickness (Figure 29). It was evaluated that at 160 °C the growth rate was at first 0.11 Å/cycle but increased up to 0.75 Å/cycle between the 3000 and 4000 cycles. This increase of the growth rate was explained by the catalytic activity of Au in the same manner as when $BH_3(NHMe_2)$ was applied to the thermal Ag process (Chapter 4.1).[V]

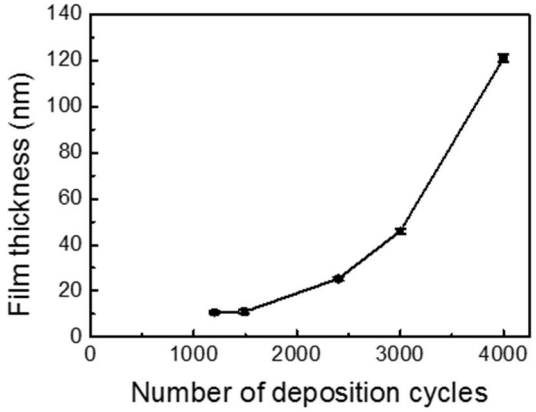

Figure 29. The Au thin film thickness as a function of the number of the deposition cycles. These Au thin films were deposited at 160 °C. Reprinted from Journal of Vacuum Science and Technology A, vol. 35, page 01B112, M. Mäkelä et al.: "Potential gold(I) precursors evaluated for atomic layer deposition", Copyright (2012), reproduced with permission from AIP Publishing LLC (American Vacuum Society).
http://avs.scitation.org/doi/abs/10.1116/1.4968193?journalCode=jva

The observed decrease in the growth rate of Au at 100 and 120 °C when applying increasing number of cycles was finally explained by a passivation of the Au surface with PEt_3. This was also supported by the fact that all the tested

co-reactants including O_3 resulted in very low growth rates. Another explanation considered was the passivation of the surface with hexamethyldisilazane, $HN(SiMe_3)_2$, which is a possible byproduct of the reactions. On oxide surfaces $HN(SiMe_3)_2$ can react with the isolated OH-groups and form -$OSiMe_3$ groups which block chemisorption sites from the precursors. However, it is believed that $HN(SiMe_3)_2$ should not passivate metallic Au particles.[103] Hence, the growth should proceed faster on Au than on Si after a nucleation period. Also, when O_3 was applied, O_3 would have combusted the passivating -$OSiMe_3$ groups. To study possible -PEt_3 (and -$OSiMe_3$) impurities on Au surface, one particulate Au thin film deposited on Ru at 120 °C was analyzed by TOF-ERDA. Analysis showed that there were no signs of Si or P on Au. TOF-ERDA thus did not prove the hypothesis of passivating groups on the surface. It can be proposed that some other characterization method (like X-ray photoelectron spectroscopy) would be more sensitive to detect a monolayer of the impurities.

Similar to the experiments performed while developing the thermal Ag ALD process, the effect of Ru to $BH_3(NHMe_2)$ was studied in this gold process too. When Ru pieces were placed in the substrate holder in front of the Si(100) substrate, the growth rate increased from 0.055 Å/cycle to 0.082 Å/cycle on Si when equal number of cycles were applied at 120 °C. When Ru was inserted to the source tube of $BH_3(NHMe_2)$, the growth rate increased further to 0.10 Å/cycles. In the chamber Ru became at least partly covered with Au whereas in the source tube it remained uncoated as it was in contact with only $BH_3(NHMe_2)$. It was concluded that at 120 °C Ru is catalytically more active than Au. Interestingly it was also noticed that pulsing of H_2S as a third precursor lowered the growth rate of Au in the process of $Au(N(SiMe_3)_2)(PEt_3)$ and $BH_3(NHMe_2)$. H_2S was pulsed before the other precursors with the idea to derivatize the Au surface with SH-groups that would attract $Au(N(SiMe_3)_2)(PEt_3)$. By contrast the growth rate of Au decreased from 0.10 Å/cycles to 0.03 Å/cycle at 160 °C when the same number of cycles were applied. It seems that SH-groups, if forming, poisoned the catalytic Au surface.[5]

Apart from the thick films deposited at 160 °C, the deposited Au thin films consisted of isolated particles (Figure 30a). The Au thin films deposited at 160 °C to nominal thicknesses of 46 and 120 nm were continuous (Figure 30b). At 160 °C the metal precursor decomposed more extensively which may explain the difference in the film microstructure. Below 160 °C it is likely that the particulate appearance of Au originated from the surface selective reduction mechanism when using $BH_3(NHMe_2)$ as a reducing agent. Like in the thermal Ag process where $BH_3(NHMe_2)$ was more likely to reduce chemisorbed metal precursor on Ag particles, $BH_3(NHMe_2)$ seems to reduce chemisorbed Au precursor on Au particles more effectively than on bare Si. Minor decomposition of the Au precursor may be required to start the growth by offering the catalytic sites. All the deposited thin films were concluded to be polycrystalline and consisted of the cubic phase of gold.[V]

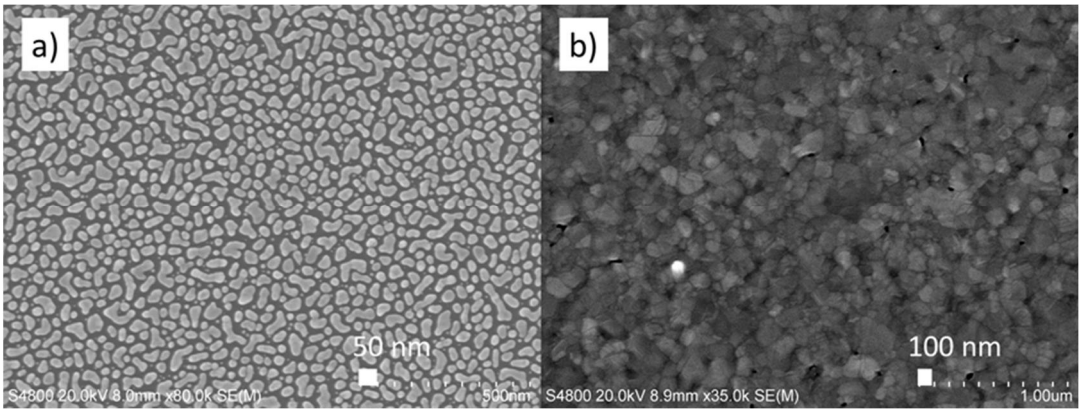

Figure 30. FESEM images of the Au thin films deposited from $Au(N(SiMe_3)_2)(PEt_3)$ and $BH_3(NHMe_2)$ at a) 100 °C with 1000 cycles (film thickness 7.5 nm) b) 160 °C with 4000 cycles (film thickness 120 nm). Both thin films were deposited with 1 s $Au(N(SiMe_3)_2)(PEt_3)$ and 1 s $BH_3(NHMe_2)$ pulses. Image modified from Journal of Vacuum Science and Technology A, vol. 35, page 01B112, M. Mäkelä et al.: "Potential gold(I) precursors evaluated for atomic layer deposition", Copyright (2012), reproduced with permission from AIP Publishing LLC (American Vacuum Society).
http://avs.scitation.org/doi/abs/10.1116/1.4968193?journalCode=jva

As a consequence of the particulate structure and large gaps between the islands, most of the Au thin films were non-conductive. Only the two thickest films deposited at 160 °C were continuous and conductive. A mean resistivity

for a film having a mean thickness of 46 nm was 5.3 μΩ·cm, and for a film with a mean thickness of 120 nm it was 3.8 μΩ·cm. It must be emphasized that these films were non-uniform in thickness.[V] As a comparison the resistivities of the 40 – 47 thick thin films deposited by thermal ALD from $Me_2Au(S_2CNEt_2)$ and O_3 were in the range of 4 – 17 μΩ·cm.[IV] This shows that the resistivity values achieved at 160 °C with the process of $Au(N(SiMe_3)_2)(PEt_3)$ and $BH_3(NHMe_2)$ are on a good low level although $Au(N(SiMe_3)_2)(PEt_3)$ decomposed to somewhat.

The chemical composition of a Au thin film deposited with 1 s pulses at 160 °C on Si was analyzed by TOF-ERDA. This continuous Au film was 120 nm thick and contained 96 at.% Au, 2 at.% O, 1 at.% H, 0.8 at.% C, 0.06 at.% N and 0.3 at.% P. The result showed that the impurity contents were low in the analyzed Au thin film although $Au(N(SiMe_3)_2)(PEt_3)$ decomposed thermally to somewhat at this temperature. It can also be concluded that no B was found from any of the thin films deposited by using $BH_3(NHMe_2)$ as a reducing agent. This is valid also for the $Ag(fod)(PEt_3)$ and $BH_3(NHMe_2)$ process.

4.3 Application of the developed Ag PEALD process to two case studies

4.3.1 Case study 1: Surface Enhanced Raman Spectroscopy

Three-dimensionally structured SERS substrates were coated with PEALD Ag. The SERS substrates were prepared with electron beam lithography and reactive-ion etching, and consisted of periodical nanopillars which were 300 nm high. Diameters of the nanopillars varied between 70 – 288 nm and the interpillar separations were between 85 – 298 nm. The nanopillars covered a square area with a side length of 20 – 60 μm.[VI] These structures were considered optimal for a SERS substrate because the sample preparation was easy, there were long-range periodic structures and it was expected that plasmonic “hot-spots” are created between the nanopillars when coated with

Ag. These hot-spots are plasmonic effects, which occur when e.g. plasmonic nanoparticles are close to each other. Only a few nm separations are desired. In the hot-spots electromagnetic fields are amplified by several orders of magnitude and single-molecule SERS is possible.[VI] It is desired that the number of hot-spots on a SERS substrate is as high as possible leading to a high probability of a single molecule to fall within the hot spot region.[VI,104-107]

Test structures were successfully coated with PEALD Ag (Figure 31). SERS measurements were done on thiophenol which was applied on the Ag surface right after the deposition. Several Raman spectra were measured: from a neat thiophenol solution, from the self-assembled monolayer (SAM) of thiophenol on the Ag surface without the nanopillars, and from the SAM of thiophenol on the Ag surface with the nanopillars. It should be noticed that the Ag surface deposited by PEALD is inherently suitable for SERS because of the island-like surface structures. Still the results showed that the strongest Raman spectra were recorded from the structures where the nanopillar gaps were less than 20 nm. The weakest Raman spectrum was measured from a neat solution.[VI]

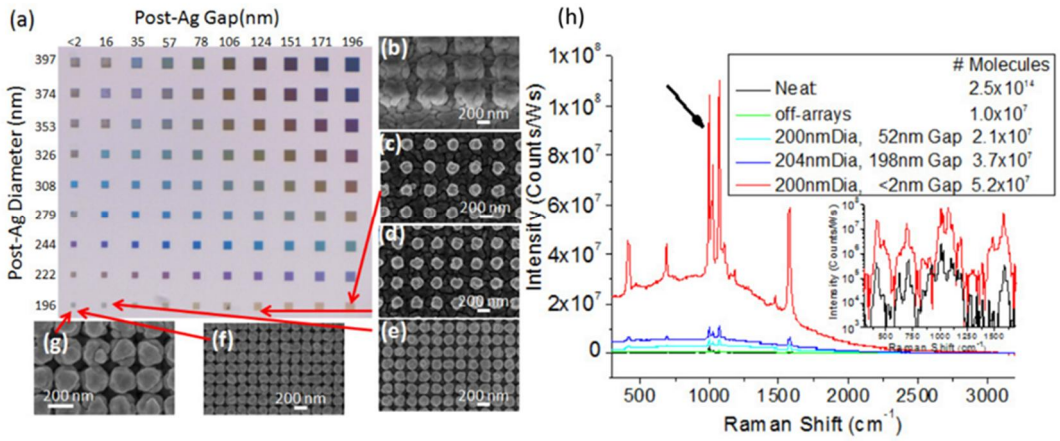

Figure 31. a) Optical reflection image of a single SERS substrate coated with PEALD Ag. On the x-axes interpillar gaps after the PEALD coating are shown. On the y-axes the diameters of the pillars after the PEALD coating are shown. b) Tilted-view SEM image of the coated nanopillars. c-f) top-view images of the interpillars having a diameter of ~196 nm with (c) separation of 196 nm, (d) 124 nm, (e) 16 nm and (f) < 2 nm g) a closer look on the pillars with < 2 nm separation. h) measured Raman spectra. Black line: a neat thiophenol solution, green line: SERS spectrum measured from the SAM of thiophenol on the PEALD Ag surface without the test structures and red, light blue and dark blue line: three SERS spectra measured from the SAM of thiophenol on the test structures coated with PEALD Ag. Permission from etc. Reprinted from Optics Express, vol. 19, pages 26056-26064, J. D. Caldwell et al.: "*Large-area plasmonic hot-spot arrays: sub-2 nm interparticle separations with plasma-enhanced atomic layer deposition of Ag on periodic arrays of Si nanopillars*", Copyright (2011), reproduced with permission from OSA Publishing. https://www.osapublishing.org/oe/abstract.cfm?uri=oe-19-27-26056

The advantage of applying PEALD (or thermal ALD) to a production of SERS substrates is that the thickness of a metal coating can be precisely controlled because of the self-limiting nature of the ALD growth. By tuning the cycle number, the separations between the structures can be controlled to create hot-spots. In the paper VI it was concluded that by applying ALD to preparation of SERS substrates interparticle separations less than 10 nm can be reproducibly made. Other advantage of applying ALD to the preparation of SERS substrates is conformality of the ALD coating.

4.3.2 Case study 2: Titanium implants

For medical implant applications the PEALD process of Ag thin films was used. Ti implants which had TiO_2 nanotubes and nanoneedles on the surface were coated. TiO_2 nanotubes were made on Ti by electrochemical oxidation with voltages ranging from 3 – 20 V and TiO_2 nanoneedles with thermal oxidation at temperatures of 475 and 500 °C in reduced pressure under. Structurally these samples resemble implants which are used in osteointegration.[VII] Osteointegration is a structural linkage used e.g. in dentistry when a synthetic dental implant is fixed to the human bone of the jaw.[108] To this implant a dental prosthesis is connected.[109] The nanostructures, nanotubes and nanoneedles, on Ti resemble morphology of a natural extra-cellular matrix and ensured high surface to volume ratio which is beneficial in implementation.[VII] In this study additional antimicrobial activity was desired from the implants and that was the reason for the Ag coating. There is increasing interest towards modifying implants to be antimicrobial because of the increasing antibiotic resistance.[VII] It is known that TiO_2 nanotubes can be antimicrobial inherently and the nanotube diameter and the crystal phase affect the antimicrobial response.[110,111] To secure or to strengthen the antimicrobial activity, these Ti samples were coated with Ag nanoparticles. In the case of Ag nanoparticles, it has been shown that their size and shape affect the antibacterial properties. One study showed that the smaller the Ag nanoparticles, the more effective their antimicrobial response.[112]

The samples were successfully coated with the PEALD Ag. On every sample either 25, 50, 100, 150 or 200 cycles of PEALD Ag were applied. It seemed that the nucleation of Ag was different on the nanoneedle and on the nanotube samples. On the nanoneedles the Ag nanoparticles were always more dispersed (Figure 32a) than on the nanotubes where the coverage of the Ag nanoparticles was larger (Figure 32b). Ag nanoparticles covered completely the nanotube samples with tube diameters of 10 – 35 nm when 150 and 200 cycles of PEALD Ag were applied i.e. no tube structures were visible under the

Ag coating. The samples chosen for the biological experiments had a tube diameter over 35 nm and a Ag coating deposited with 25 cycles (Figure 32c). The expectation was that the best antimicrobial response should be obtained with the smallest Ag nanoparticles as introduced above.[VII]

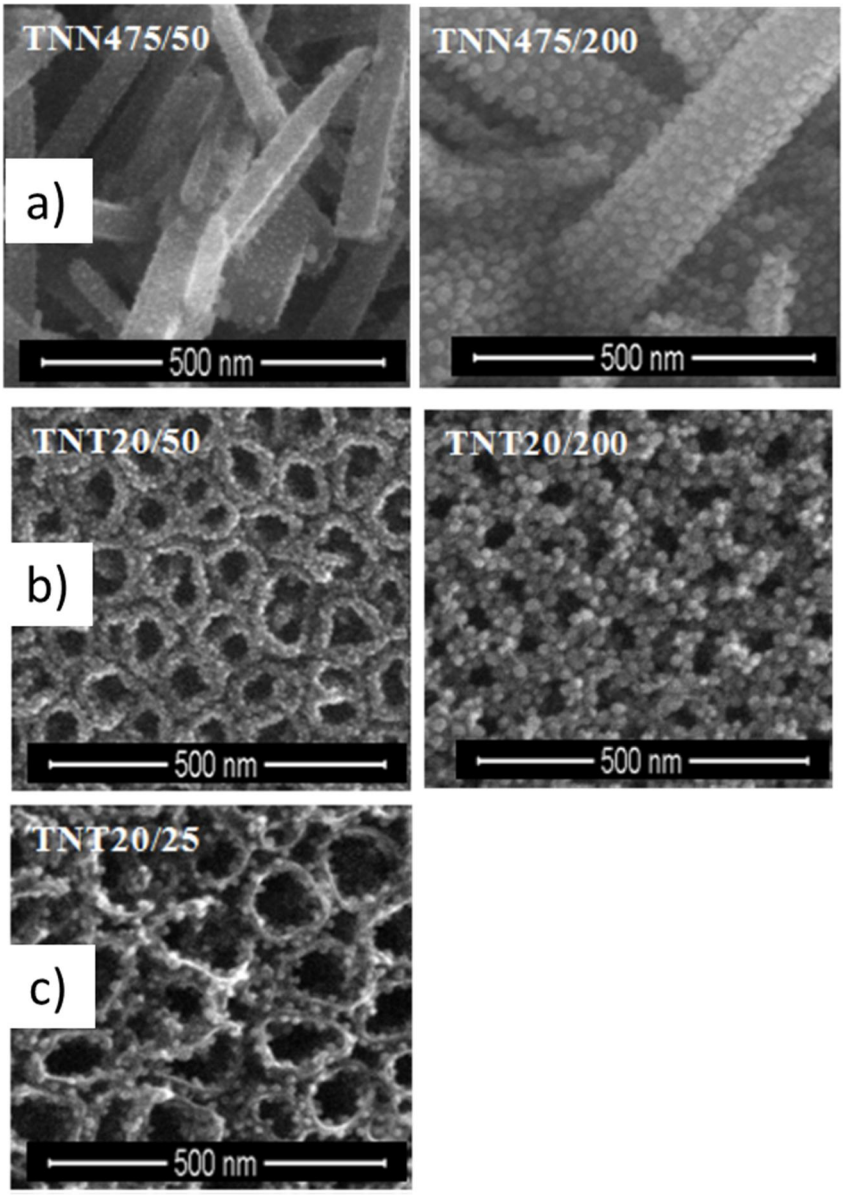

Figure 32. a) Nanoneedle samples prepared at 475 °C. left: 50 PEALD Ag cycles were applied, right: 200 PEALD Ag cycles. b) Nanotube samples prepared with a voltage of 20 V. The tube diameter is 77 – 84 nm. left: 50 PEALD Ag cycles, right: 200 PEALD cycles. c) One of the nanotube samples chosen for the biological experiments. This sample was prepared with a voltage of 20 V and 25 PEALD Ag cycles. Image from Nanomaterials, vol. 7, pages 26056-26064, A. Radtke et al.: "*Optimization of the Silver Nanoparticles PEALD Process on the Surface of 1-D Titania Coatings*, Copyright (2017). https://www.ncbi.nlm.nih.gov/pmc/articles/PMC5535259/

It was concluded that the Ag nanoparticle size increased when more PEALD cycles were applied. It also seemed that the nanoparticle size was independent of the nanotube diameter. Biological experiments showed that all the samples enhanced fibroblast proliferation as compared to the Ti implants without any TiO_2 structures or PEALD Ag. Fibroblast proliferation is important in wound healing because the fibroblast cells, which are the main cellular components of connective tissues, synthesize extracellular matrix.[113] The samples where the nanotube diameter was smaller showed stronger fibroblast proliferation compared to the samples where the nanotube diameter was larger. To study antimicrobial activity of the samples bacteria (Staphylococcus aureus) were applied on them. The bacteria were applied either by suspension method or topically. In the suspension method the samples were held for 24 h in a bacterial suspension. In the topical method 40 µL of bacterial suspension was topically applied on the samples.[VII] All the implants with nanotube structures coated with PEALD Ag showed antimicrobial activity when the bacteria were applied by the suspension method. However, in most cases no antimicrobial effect was noticed when the bacteria were applied topically on the implants with TiO_2 nanotubes coated with PEALD Ag. In this case antimicrobial effect was noticed only in the implant with the smallest diameter nanotubes coated with PEALD. Several reasons for the observed difference were discussed, e.g. when applied topically the bacteria might have had limited contact with the Ag nanoparticles.[VII]

5 CONCLUSIONS

During this thesis work, new ALD processes were developed for Ag and Au thin films. In the literature only a few ALD processes for these metals exist although there are many potential applications in the field of photonics, electronics, catalysis and biosciences. The main problem has been the lack of suitable metal precursors. Silver and gold compounds are often thermally unstable and hence unsuitable for ALD. During this work several silver and gold compounds were evaluated for ALD. Most of the compounds showed limited thermal stability, as expected. One Ag, one Au(I) and one Au(III) compound were chosen for the ALD experiments.

A PEALD process was developed for Ag thin films where Ag(fod)(PEt_3) and plasma-activated H_2 were applied. The ALD temperature range was narrow between 120 – 140 °C because of the high evaporation temperature (106 °C) and relatively low thermal stability of the Ag precursor. The Ag thin films were polycrystalline showing the cubic phase of silver. The resistivity of the continuous 22 nm thick Ag thin film was 6 – 8 μΩ·cm which is a very good value for an ALD thin film. Ag(fod)(PEt_3) was also applied in thermal ALD with $BH_3(NHMe_2)$ as a reducing agent to produce particulate Ag thin films. This process showed self-limiting growth at 110 °C in respect to the Ag(fod)(PEt_3) pulse but not in respect to the $BH_3(NHMe_2)$ pulse.

Two Au precursors were tested for thermal ALD. The Au(III) compound, $Me_2Au(S_2CNEt_2)$, showed self-limiting growth at 180 °C when used with O_3. Thermal decomposition was noticed only at 250 °C. The Au thin films deposited were continuous and conductive. Resistivities of 40 – 47 nm thick Au thin films deposited at 180 °C were 4.5 – 17 μΩ·cm. The Au thin films were found pure by TOF-ERDA and consisted of the cubic phase of gold. The problem of the process was very low synthesis yield of $Me_2Au(S_2CNEt_2)$, but a clear benefit was the usage of O_3 because it is a general co-reactant in ALD.

The studied Au(I) precursor, $Au(N(SiMe_3)_2)(PEt_3)$, was easy to synthesize with high yields but no true self-limiting growth was confirmed with $BH_3(NHMe_2)$ which was applied as a reducing agent. Several other potentially reducing co-reactants were also tested to find new reducing agents to ALD, but $BH_3(NHMe_2)$ was still found to be the best choice. Even though no ALD was confirmed, the process produced pure Au coatings in a controllable way.

During this thesis work it was confirmed that catalytic surfaces like Ag and Au can convert $BH_3(NHMe_2)$ to more reducing species, possibly $[Me_2N\text{-}BH_2]_2$. In addition to the deposited catalytic surfaces, $BH_3(NHMe_2)$ could be activated already in the source tube by placing Ru pieces there. This shows that the new species produced from $BH_3(NHMe_2)$ are volatile enough to be transported through the gas phase.

In the two case studies the PEALD process of Ag was applied to potential applications. In the first one, nanostructured SERS substrates were coated. Noticeable enhancements in the SERS response were seen with the test structures having the Ag coating. In the second study, titanium implants modified with either thermal or electrochemical oxidation were coated with Ag. It was concluded that the Ag coated implants enhanced fibroblast proliferation which is important in wound healing. The Ag coated implants also gained antimicrobial activity compared to the unmodified implants. In both studies the main advantage of applying ALD to the preparation of the samples was that the amount of Ag was well controlled because of the self-limiting nature of the PEALD Ag growth.

6 REFERENCES

[1] Z. Zhang, M. G. Lagally, *Science* 276 (1997) 377.

[2] V. Miikkulainen, M. Leskelä, M. Ritala, R. L. Puurunen, *J. Appl. Phys.* 113 (2013) 021301.

[3] M. Leskelä, M. Ritala, *Thin Solid Films* 409 (2002) 138.

[4] R. Puurunen, *J. Appl. Phys.* 97 (2005) 121301.

[5] H. B. Profijt, S. E. Potts, M. C. M. van de Sanden, W. M. M. Kessels, *J. Vac. Sci. Technol. A*. 29 (2011) 050801.

[6] A. Niskanen, T. Hatanpää, K. Arstila, M. Leskelä, M. Ritala, *Chem. Vap. Deposition* 13 (2007) 408.

[7] F. J. van den Bruele, M. Smets, A. Illiberi, Y. Creyghton, P. Buskens, F. Roozeboom, P. Poodt, *J. Vac. Sci. Technol. A.* 33 (2015) 01A131.

[8] A. A. Amusan, B. Kalkofen, H. Gargouri, K. Wandel, C. Pinnow, M. Lisker, E. P. Burte, *J. Vac. Sci. Technol. A.* 34 (2016) 01A126.

[9] M. M. Minjauw, E. Solano, S. P. Sree, R. Asapu, M. Van Daele, R. K. Ramachandran, G. Heremans, S. W. Verbruggen, S. Lenaerts, J. A. Martens, C. Detavernier, J. Dendooven, *Chem. Mater*. 29 (2017) 7114.

[10] M. B. E. Griffiths, P. J. Pallister, D. J. Mandia, S. T. Barry, *Chem. Mater.* 28 (2016) 44.

[11] C. Burda, X. Chen, R. Narayanan, M. A. El-Sayed, *Chem. Rev.* 105 (2005) 1025.

[12] P. L. Stiles, J. A. Dieringer, N. C. Shah, R. P. Van Duyne, *Annu. Rev. Anal. Chem.* 1 (2008) 601.

[13] X. Huang, M. A. El-Sayed, *J. Adv. Res.* 1 (2010) 13.

[14] K. Knapas, M. Ritala, *Crit. Rev. Solid State Mater. Sci.* 38 (2013) 167.

[15] S. M. George, *Chem. Rev.* 110 (2010) 111.

[16] T. Aaltonen, P. Alen, M. Ritala, M. Leskelä, *Chem. Vap. Deposition* 9 (2003) 45.

[17] T. Aaltonen, M. Ritala, K. Arstila, J. Keinonen, M. Leskelä, *Chem. Vap. D*eposition 10 (2004) 215.

[18] T. Aaltonen, M. Ritala, V. Sammelselg, M. Leskelä, *J. Electrochem. Soc.* 151 (2004) G489.

[19] J. Hämäläinen, M. Ritala, M. Leskelä, *Chem. Mater.* 26 (2014) 786.

[20] R. W. Johnson, A. Hultqvist, S. F. Bent, *Mater. Today* 17 (2014) 236.

[21] R. Puurunen, *Chem. Vap. Deposition* 20 (2014) 332.

[22]https://beneq.com/en/displays/blog/ald-in-extreme-conditions-0, accessed 8th of Dec., 2017

[23] E. Salmi (2015), *Atomic Layer Deposited Coatings fo Corrosion Protection of Metals. Academic Dissertation.*, University of Helsinki. https://helda.helsinki.fi/handle/10138/156985

[24] T. J. Knisley, L. C. Kalutarage, C. H. Winter, *Coord. Chem. Rev.* 257 (2013) 3222.

[25] T. Hatanpää, M. Ritala, M. Leskelä, *Coord. Chem. Rev.* 257 (2013) 3297.

[26] A. Niskanen, T. Hatanpää, M. Ritala, M. Leskelä, *J. Therm. Anal. Calorim.* 64 (2001) 955.

[27] A. Niskanen (2006), *Radical Enhanced Atomic Layer Deposition of Metals and Oxides.*, University of Helsinki.

https://helda.helsinki.fi/handle/10138/21033

[28] A. Niskanen, A. Rahtu, T. Sajavaara, K. Arstila, M. Ritala, M. Leskelä*, J. Electrochem. Soc.* 152 (2005) G25.

[29] A. Niskanen, K. Arstila, M. Leskelä, M. Ritala, *Chem. Vap. Deposition* 13 (2007) 152.

[30] A. Niskanen, K. Arstila, M. Ritala, M. Leskelä, *J. Electrochem. Soc.* 152 (2005) F90.

[31] A. Niskanen, U. Kreissig, M. Leskelä, M. Ritala, *Chem. Mater.* 19 (2006) 2316.

[32] A. Bogaerts, E. Neyts, R. Gijbels, J. van der Mullen, *Spectrochim. Acta Part B* 57 (2002) 609.

[33] J. Kim, S. Kim, H. Kang, J. Choi, H. Jeon, M. Cho, K. Chung, S. Back, K. Yoo, C. Bae, *J. Appl. Phys*. 98 (2005) 094504.

[34] J. Kim, S. Kim, H. Jeon, M.-H. Cho, K.-B. Chung, C. Bae, *Appl. Phys. Lett.* 87 (2005) 053108.

[35] H. B. Projfit, W. M. M. Kessels, *ECS Trans.* 50 (2013) 23.

[36] Personal communication from Mr. Markus Bosund, Beneq Oy.

[37] B. H. Lee, S. Cho, J. K. Hwang, S. U. Kim, M. M. Sung, *Thin Solid Films* 518 (2010) 6432.

[38] H. B. Profijt, P. Kudlacek, M. C. M. van de Sanden, W. M. M. Kessels, *J. Electrochem. Soc.* 158 (2011) G88.

[39] S. Samukawa, M. Hori, S. Rauf, K. Tachibana, P. Bruggeman, G. Kroesen, J. C. Whitehead, A. B. Murphy, A. F. Gutsol, S. Starikovskaia, U. Kortshagen, J.-P. Boeuf, T. J. Sommerer, M. J. Kushner, U. Czarnetzki, N. J. Mason*, Phys. D: Appl. Phys.* 45 (2012) 253001.

[40] S. P. Krumdieck (2009) *CVD Reactors and Delivery System Technology.* In A. C. Jones and M. L. Hitchman (Ed.), Chemical Vapor Deposition: Precursors Processes and Applications (pages 37-92). The Royal Society of Chemistry, Cambridge, UK 2009.

[41] H. C. M. Knoops, E. Langereis, M. C. M. van de Sanden, W. M. M. Kessels, *J. Electrochem. Soc.* 157 (2010) G241.

[42] J. Dendooven, D. Deduytsche, J. Musschoot, R. L. Vanmeirhaeghe, C. Detavernier, *J. Electrochem. Soc.* 157 (2010) G111.

[43] J. C. Greaves, J. W. Linnett, *Trans. Faraday Soc.* 55 (1959) 1346.

[44] S. B. S. Heil, J. L. van Hemmen, M. C. M. van de Sanden, W. M. M. Kessels, *J. Appl. Phys.* 103 (2008) 103302.

[45] M. Napari (2017), *Low-temperature thermal and plasma-enhanced atomic layer deposition of metal oxide thin films. Academic Dissertation.*, University of Jyväskylä.

https://jyx.jyu.fi/dspace/handle/123456789/55140

[46] S. Sneck, M. Söderlund, M. Bosund, P. Soininen, Conference paper in Semiconductor Technology International Conference (CSTIC), 2017 China. 12-13 March 2017. http://ieeexplore.ieee.org/document/7919810/#

[47] D. Munoz-Rojas, J. MacManus-Driscoll, *Mater. Horizons* 1 (2014) 314.

[48] V. Amendola, R. Pilot, M. Frasconi, O. M. Maragó, M.A. Iati, *J. Phys. Condens. Matter* 29 (2017) 203002.

[49] ThoughtCo. *Table of electrical resistivity and conductivity, flow of current through materials* by Anne Marie Helmenstine, https://www.thoughtco.com/table-of-electrical-resistivity-conductivity-608499, accessed 5th of Dec., 2017.

[50] R. Yan, D. Gargas, P. Yang, *Nat. Photonics* 3 (2009) 569.

[51] H. Van Bui, F. Grillo, J. R. van Ommen, *Chem. Comm.* 53 (2017) 45.

[52] H. Liu, B. Wang, E. S. P. Leong, P. Yang, Y. Zong, G. Si, J. Teng, S. A. Maier, *ACS Nano* 4 (2010) 3139.

[53] S. Link, M. A. El-Sayed, *Int. Rev. Phys. Chem.* 19 (2000) 409.

[54] A. Campion, P. Kambhampati, *Chem. Soc. Rev.* 27 (1998) 241.

[55] S. Lal, S. Link, N. J. Halas, *Nat. Photonics* 1 (2007) 641.

[56] W. L. Barnes, A. Dereux, T. W. Ebbesen *Nature* 424 (2003) 824.

[57] H. Im, N. C. Lindquist, A. Lesuffleur, S.-H. Oh, *ACS Nano* 4 (2010) 947.

[58] J. Fontana, J. Livenere, F. J. Bezares, J. D. Caldwell, R. Rendell, *Appl. Phys. Lett.* 102 (2013) 201606.

[59] A. P. Piedade, M. T. Vieira, A. Martins, F. Silva, *Nanotechnology* 18 (2007) 105103.

[60] D. J. Balazs, K. Triandafillu, P. Wood, Y. Chevolot, C. van Delden, H. Harms, C. Hollenstein, H. J. Mathieu, *Biomaterials* 25 (2004) 2139.

[61] A. Remes, D. F. Williams, *Biomaterials* 12 (1991) 607.

[62] T. Hanawa, M. Kaga, Y. Itoh, T. Echizenya, H. Oguchi, M. Ota, *Biomaterials* 13 (1992) 20.

[63] J. J. Blaker, S. N. Nazhat, A. R. Boccaccini, *Biomaterials* 25 (2004) 1319.

[64] H. J. Mueller, *Dent. Mater.* 17 (2001) 60.

[65] T. Aaltonen, M. Ritala, T. Sajavaara, J. Keinonen, M. Leskelä, *Chem. Mater.* 15 (2003) 1924.

[66] H. Shi, R. Asahi, C. Stampfl, *Phys. Rev. B* 75 (2007), 205125.

[67] J. J. Senkevich, F. Tang, D. Rogers, J. T. Drotar, C. Jezewski, W. A. Lanford, G.-C. Wang, T.-M. Lu, *Chem. Vap. Deposition* 9 (2003) 258.

[68] G. A. Ten Eyck, S. Pimanpang, H. Bakhru, T.-M. Lu, G.-C. Wang, *Chem. Vap. Deposition* 12 (2006) 290.

[69] M. J. Weber, A. J. M. Mackus, M. A. Verheijen, C. van der Marel, W. M. M. Kessels, *Chem. Mater.* 24 (2012) 2973.

[70] J. W. Elam, A. Zinovev, C. Y. Han, H. H. Wang, U. Welp, J. N. Hryn, M. J. Pellin, *Thin Solid Films*, 515 (2006) 1664.

[71] H. Feng, J. W. Elam, J. A. Libera, W. Setthapun, P. C. Stair, *Chem. Mater.* 22 (2010) 3133.

[72] Sigma-Aldrich (Merck), MSDS of Si_2H_6: http://www.sigmaaldrich.com/MSDS/MSDS/DisplayMSDSPage.do?country=FI&language=fi&productNumber=463043&brand=ALDRICH&PageToGoToURL=http%3A%2F%2Fwww.sigmaaldrich.com%2Fcatalog%2Fproduct%2Faldrich%2F463043%3Flang%3Dfi accessed 13th of Dec. 2017

[73] Praxair, MSDS of B_2H_6: http://www.praxair.com/-/media/documents/sds/diborane-b2h6-safety-data-sheet-sds-p4586.pdf accessed 13th of Dec. 2017

[74] J. P. Klesko, C. M. Thrush, C. H. Winter, *Chem. Mater.* 27 (2015) 4918.

[75] T. Saito, H. Nishiyama, H. Tanahashi, K. Kawakita, H. Tsurugi, K. Mashima, *J. Am. Chem. Soc.* 136 (2014) 5161.

[76] L. C. Kalutarage, P. D. Martine, M. J. Heeg, C. H. Winter, *J. Am. Chem. Soc.* 135 (2013) 12588.

[77] L. C. Kalutarage, S. B. Clendenning, C. H. Winter, *Chem. Mater.* 26 (2014) 3731.

[78] T. Watanabe, S. Hoffmann-Eifert, R. Waser, C. S. Hwang, 2007 Sixteenth IEEE International Symposium on the Applications of Ferroelectrics, Nara, 2007, 156.

[79] P. R. Chalker, S. Romani, P. A. Marshall, M. J. Rosseinsky, S. Rushworth, P. A. Williams, *Nanotechnology* 21 (2010) 405602.

[80] Z, Golrokhi, S. Chalker, C. J. Sutcliffe, R. Potter, *Appl. Surf. Sci.* 364 (2016) 789.

[81] Z. Golrokhi, P. A. Marshall, S. Romani, S. Rushworth, P. R. Chalker, R. Potter, *Appl. Surf. Sci.* 399 (2017) 123.

[82] S. S. Masango, L. Peng, L. D. Marks, R. P. Van Duyne, P. C. Stair, *J. Phys. Chem. C.* 118 (2014) 17655.

[83] A. Grodzicki, I. Lakomska, P. Piszczek, I. Szymanska, E. Szlyk, *Coord. Chem. Rev.* 249 (2005) 2232.

[84] R. Parkhomenko, A. Alexeyev, N. Morozova, I. Igumenov, *J. Coord. Chem.* 65 (2012) 3227.

[85] A. E. Turgambaeva, G. I. Zharkova, P. P. Semyannikov, V. V. Krisyuk, T. P. Koretskaya, S. V. Trubin, B. V. Kuchumov, I. K. Igumenov, *Gold Bull.* 44 (2011) 177.

[86] T. Suntola, *Thin Solid Films* 216 (1992) 84.

[87] R. A. Waldo, in Microbeam Anal. Newbury, D. E. Ed.; San Francisco Press; San Francisco, CA, 1988; pp 310-314.

[88] M. Putkonen, T. Sajavaara, L. Niinistö, J. Keinonen, *J. Anal. Bioanal. Chem.* 382 (2005) 1791.

[89] C. A. Jaska, K. Temple, A. J. Lough, I. Manners, *J. Am. Chem. Soc.* 125 (2003) 9424.

[90] J. Lu, J. W. Elam, P. C. Stairs, *Surf. Sci. Rep.* 71 (2016) 410.

[91] S. D. Elliot, G. Dey, Y. J. Maimati, *J. Chem. Phys.* 146 (2017) 052822.

[92] Z. Yuan, N. H. Dryden, J. J. Vittal, R. J. Puddephatt, *Chem. Mater.* 7 (1995) 1696.

[93] L. Gao, P. Härter, Ch. Linsmeier, A. Wiltner, R. Emling, D. Schmitt-Landsiedel, *Microelectron. Eng.* 82 (2005) 296.

[94] A. F. Mayadas, M. Shatzkes, *Phys. Rev. B* 1 (1970) 1382

[95] J. W. C. De Vries, *Thin Solid Films* 167 (1988) 25.

[96] M. O. Faltens, D. A. Shirley, *J. Chem. Phys.* 53 (1970) 4249.

[97] V. M. Gurevich, K. S. Gavrichev, V. E. Gorbunov, N. N. Baranova, B. R. Tagirov, L. N. Golushina, V. B. Polyakov, *Thermochim. Acta* 412 (2004) 85.

[98] P. D. Tran, P. Doppelt, *J. Electrochem. Soc.* 154 (2007) D520.

[99] E. Feurer, H. Suhr, *Appl. Phys. A.* 44 (1987) 171.

[100] F. E. Beamish, J. J. Russell, J. Seath, *Ind. Eng. Chem. Anal. Ed.* 9 (1937) 174.

[101] S. D. Perrault, W. C. W. Chan, *J. Am. Chem. Soc.* 131 (2009) 17042.

[102] S. Yagi, N. Oeda, C. Kojima, *J. Electrochem. Soc.* 159 (2012) H668.

[103] A. Jain, A. V. Gelatos, T. T. Kodas, M. J. Hempden-Smith, R. Marsh, C. J. Mogab *Thin Solid Films* 262 (1995) 52.

[104] J. P. Kottmann, O. J. F. Martin, *Opt. Express* 8 (2001) 655.

[105] T. Atay, J.-H. Song, A. V. Nurmikko, *Nano Lett.* 4 (2004) 1627.

[106] K. Kneipp, Y. Wang, H. Kneipp, L. T. Perelman, I. Itzkan, R. R. Dasari, M. S. Field, *Phys. Rev. Lett.* 78 (1997) 1667.

[107] S. Nie, S. R. Emore, *Science* 275 (1997) 1102.

[108] McGraw-Hill Concise Dictionary of Modern Medicine. © 2002 by The McGraw-Hill Companies, Inc. http://medical-dictionary.thefreedictionary.com/osteointegration accessed 10th Dec. 2017.

[109]https://www.colgate.com/en-us/oral-health/cosmetic-dentistry/implants/placing-dental-implants © 2002- 20182017 Aetna, Inc. Accessed 11th February 2018.

[110] D. S. Puckett, E. Taylor, T. Raimondo, T. J. Webster, *Biomaterials* 31 (2010) 706.

[111] A. Radtke, P. Piszczek, A. Topolski, Z. Levandovska, E. Talik, I. H. Andersen, L. P. Nielse, M. Heikkilä, M. Leskelä, *Appl. Sur. Sci.* 368 (2016) 165.

[112] G. A. Martinez-Castanon, N. Nino-Martinez, F. Martinez-Gutierrez, J. R. Martinez-Mendoza, F. Ruiz, F. *J. Nanopart. Res*. 10 (2008) 1343.

[113] M. Schmidt, D. Gutknecht, J. C. Simon, J.-N. Schulz, B. Eckes, U. Anderegg, A. Saalbach, *J. Investig. Dermatol.* 135 (2015) 1893.